Quaternary Geochronology 81 (2024) 101505

Contents lists available at ScienceDirect

Quaternary Geochronology

journal homepage: www.elsevier.com/locate/quageo

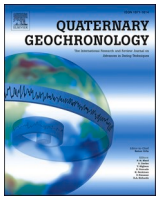

Diachronic quantification of the local marine reservoir effect (MRE) using *Loripes orbiculatus* shells from Late Holocene lagoonal deposits at Puntone di Scarlino (Central Tuscany, Italy): Proposed roles of microbial diagenesis and sedimentation rates

Jan Sevink [a,*], Michael W. Dee [b], Justyna J. Niedospial [b], Arnoud Maurer [c], Wim Kuijper [d], Ilaria Mazzini [e], Ilenia Arienzo [f], Rutger L. van Hall [a]

[a] Institute for Biodiversity and Ecosystem Dynamics (IBED), University of Amsterdam, Sciencepark 904, 1098, XH, Amsterdam, the Netherlands
[b] Centre for Isotope Research, Faculty of Science and Engineering, University of Groningen, Groningen, 9747, AG, the Netherlands
[c] Groningen Institute of Archaeology, University of Groningen, Poststraat 6, 9712, ER, Groningen, the Netherlands
[d] Naturalis Biodiversity Center, Darwinweg 2, 2333, CR, Leiden, the Netherlands
[e] Consiglio Nazionale delle Ricerche, IGAG, Area della Ricerca di Roma 1 - Montelibretti, Via Salaria km 29,300 - 00015, Monterotondo, (Rome), Italy
[f] Istituto Nazionale di Geofisica e Vulcanologia (INGV), Via Diocleziano 328, 80124, Napoli NA, Italy

ARTICLE INFO

Keywords:
Holocene
Paleoceanography
Europe
Radiogenic isotopes
Marine reservoir effect
Loripes orbiculatus
Diagenetic carbon flux

ABSTRACT

With the aim of dating the early salt production at Puntone di Scarlino (Central Tuscany, Italy) and establishing the environmental history of this coastal site, a sediment core was studied, taken from the lagoon next to the archaeological site. Diachronic radiocarbon dating of terrestrial plant macro remains and *Loripes orbiculatus* (Poli, 1795) shells, a burrowing lucinid bivalve occurring throughout the sediment cored, revealed a Marine Reservoir Effect (MRE) that varied markedly over time. Between ca. 4000 and 2500 cal BP, the △R values ranged between −50 and + 500 ^{14}Cyears, thus rendering the *Loripes* shells truly unsuited for independent radiocarbon dating. Extensive geochemical and palaeoecological study of the core and its environment showed that none of the ubiquitous explanations for this highly variable MRE, such as 'hard water' or 'upwelling old seawater', can be valid. We attribute the phenomenon to the uptake by this lucinid mollusc of 'old carbon' from the sediment column into which it had burrowed, released by diagenetic microbial decomposition processes such as methanogenesis. The age of this inorganic carbon varied, being linked to the sedimentation rate: with decreasing sedimentation rate its impact will increase, whereas at high sedimentation rates its impact will likely be minimal. Our results raise serious doubts about the suitability for radiocarbon dating of benthic fauna from shallow coastal environments and point at these diagenetic processes as potentially important sources of 'old carbon'.

1. Introduction

The Central Italian coast is known for its early salt production, starting in protohistoric times at many sites. One such site is at Puntone di Scarlino (Central Tuscany, Italy; see Fig. 1) where the process entitled *briquetage* was practiced (Aranguren et al., 2014; Sevink et al., 2020). Here, salt production probably started in the Early Iron Age and continued well into the period of the Roman Republic. Age estimates based on ceramic typology have been thwarted by the fact that the associated ceramics comprised largely the coarse ware typical of such *briquetage* sites with rather undifferentiated typology (Alessandri et al., 2019). Materials suited for absolute dating were also scarce. Terrestrial plant remains were largely absent and attempts to obtain reliable radiocarbon (^{14}C) dates on secondary carbonates formed during the salt production process, and on shells from dumps of the lagoonal sediments used in this process, were in vain (Sevink et al., 2021). For both the secondary carbonates and the shells hard water effects were ruled out.

Exploratory corings in the border zone of the adjacent lagoon showed the presence of a sequence of Late Holocene lagoonal deposits with peaty intercalations which, close to the archaeological site, was

* Corresponding author.
E-mail addresses: j.sevink@uva.nl (J. Sevink), m.w.dee@rug.nl (M.W. Dee), justyna.j.n98@gmail.com (J.J. Niedospial), a.maurer@rug.nl (A. Maurer), w.j.kuijper@gmail.com (W. Kuijper), ilaria.mazzini@igag.cnr.it (I. Mazzini), ilenia.arienzo@ingv.it (I. Arienzo), R.L.vanHall@uva.nl (R.L. van Hall).

https://doi.org/10.1016/j.quageo.2024.101505
Received 17 July 2023; Received in revised form 7 December 2023; Accepted 12 February 2024
Available online 19 February 2024

several metres thick. This sequence also contained a significant quantity and variety of marine shells. Preliminary ^{14}C dates on terrestrial plant macro remains from this sequence showed that it covered the entire period of interest, starting before 4000 cal BP and continuing well into the Roman Imperial period. This led to a palaeoecological study on a core taken from this sedimentary complex with the primary aim of establishing a^{14}C-based chronology for the salt production activities and associated changes in the land use and vegetation of the area. However, it was soon realised that this core also offered excellent possibilities for a diachronic quantification of the marine reservoir effect (MRE) using shells and terrestrial plant macro remains.

The discrepancy in ^{14}C ages between contemporaneous terrestrial and marine material, defined as the marine reservoir effect (R), has been extensively described in a major review by Alves et al. (2018). The variance between ^{14}C ages on marine samples and the marine calibration curve (Heaton et al., 2020) for samples from a specific location is

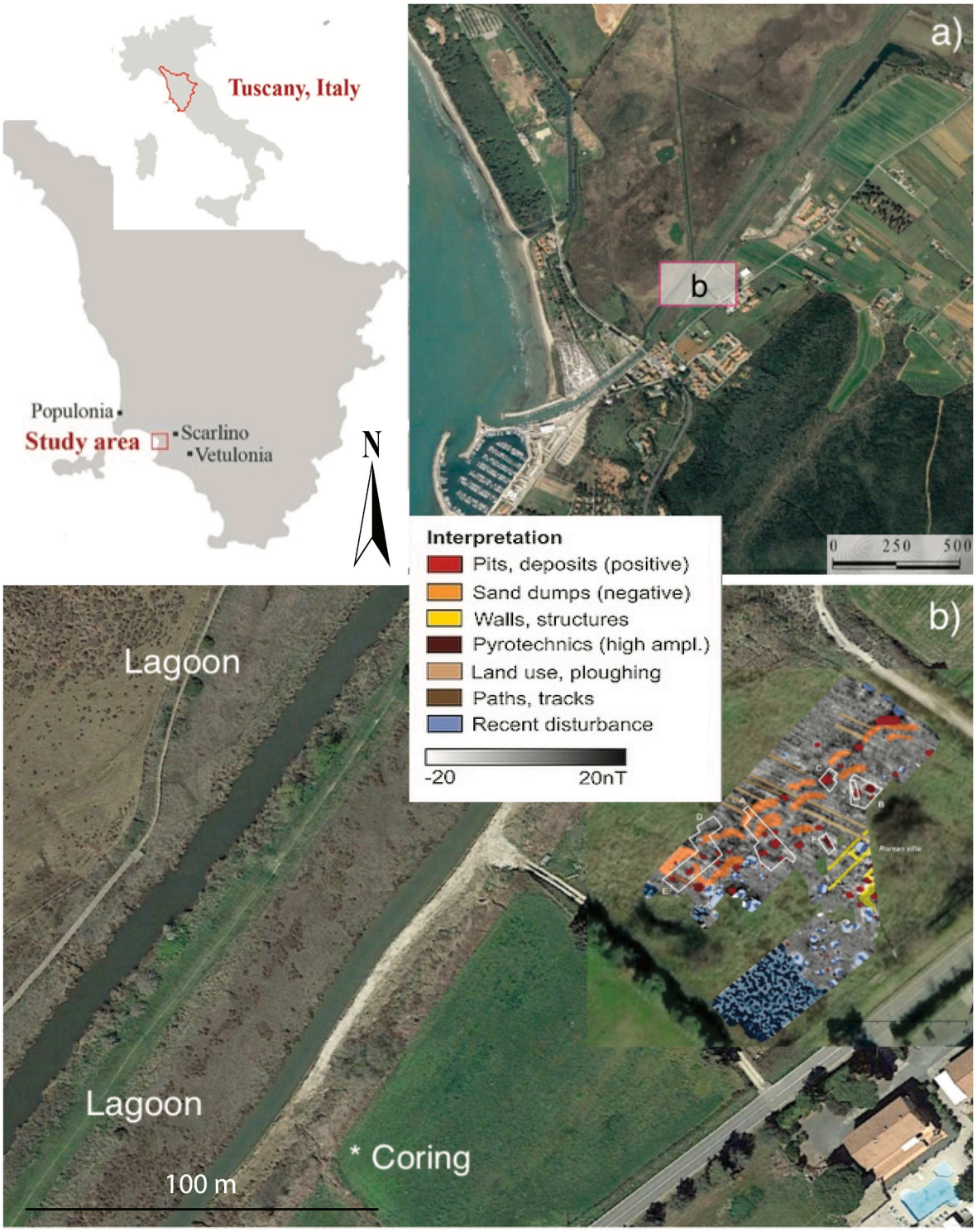

Fig. 1. The location of the study area: a) Overview of the coastal area and location of the Puntone di Scarlino site; b) Detailed map of the site (with inset of geophysics and features) and location of coring. For details of the archaeological site, see Sevink et al. (2021). Satellite images are from Google Earth.

called ΔR. This ΔR is known to be spatially quite variable but is often still considered to be rather invariant over time (Heaton et al., 2023), notably in the Mediterranean Sea because of its comparatively static nature. The ΔR value can be established either by analysing known-age marine material or paired marine-terrestrial samples. For an increasing number of locations and largely derived from the known-age approach, its magnitude is recorded in the CHRONO Marine Reservoir Database (http://calib.org/marine/), originally developed by Reimer and Reimer (2001). The calibration of ^{14}C dates on marine samples, therefore, commonly involves three parameters: the measured radiocarbon age of the sample; the global marine calibration curve (the latest being Marine20); and the local ΔR value. This latter estimate is obtained by averaging existent values recorded nearby the location in question (see Alves et al., 2018; Reimer et al., 2020). Thus, a long history already exists of examining the spatial patterning of ΔR. However, studies testing the diachronic variation for shallow coastal environments by dating a series of paired marine-terrestrial samples are scarce (Alves et al., 2018).

In this paper, the results from our diachronic study of paired, interpolated, and marine-terrestrial data for the Puntone core are reported with particular attention for the relationship between the environmental conditions (e.g., sedimentary facies) and the ΔR value. *Loripes orbiculatus* (Poli, 1795), a saltwater bivalve, was selected as the indicative species because it was the most common mollusc at the site, and the only one to be found almost right throughout our core. Results from this study that are relevant for the chronology of the salt production at Puntone will be reported in a separate paper.

2. Regional setting

The archaeological site is in the border zone of the Palude di Scarlino, on the footslope of a small alluvial fan descending from the sandstone ridge bordering the Follonica coastal plain in the south. In Fig. 1 the location of the core is indicated (42°53′30.40″N; 10°47′33.82″E), as well as the archaeological site, which has been extensively described by Sevink et al. (2020, 2021). The local geology is shown on the 1:100,000 geological map (sheet 127) and depicted in Fig. 2. The lagoon was connected to the sea till at least the mid 19th century (e.g., Cappuccini, 2011; Giroldini, 2012; Masetti et al., 2017). Sediments in the lagoon (unit p^2) are described as '*palustri attuali e recenti*', being composed of clayey to sandy lagoonal sediments of low permeability (Masetti et al., 2017). This extensive flat lagoonal plain extends far inland and merges with a very similar recent alluvial plain (unit a), described as '*alluvioni attuali e recenti*'. The Pleistocene alluvial fan complex to the south (units dt and f^2) is composed of deeply weathered sediment derived from Macigno sandstone (unit mg) and is locally covered by Holocene fan sediments (unit a). Unlike many other areas along the Tyrrhenian coast, Pleistocene marine terraces are completely absent, attesting to tectonic subsidence during the final part of the Quaternary, as also observed in the nearby Grosseto basin (e.g., Sevink et al., 1986; Lambeck et al., 2004; Biserni and Van Geel, 2005).

The Macigno formation (unit mg, Late Oligocene-Miocene) consists of grey to bluish-grey, well-consolidated, poorly to moderately sorted siliciclastic sandstone or greywacke. It may contain some calcium carbonate (generally <5%), while iron contents range from 4% to 7% Fe_2O_3 (Deneke and Gu; nther, 1981; Dinelli et al., 1999; Cornamusini, 2002). The only other relevant older geological formation is the Cretaceous to Eocene Flysch formation (unit ap) described as '*Argilloscisti silicei grigio-bruni con sfaldatura a lame sottili ('Galestri') alternati a strati di calcari silicei grigio-bruni ('Palombini'); associati si ritrovano arenaria silicee brunastre, calcari marnosi e calcareniti*'. This is a predominantly siliceous varied complex of clastic rocks with some intercalated limestone beds, occurring at a significant distance, further east and north of the site. In the east is the Gavorrano complex of Mesozoic limestones (dark blue) with a Tertiary granite intrusion (red). For further details see http://sgi.isprambiente.it/geologia100k/mostra_foglio.aspx?numero_foglio=127.

The hydrology of the Follonica coastal basin has been studied in considerable detail (Raco et al., 2015; Masetti et al., 2017; Positano and Nannucci, 2017), although the focus was firmly on the northern part of the basin and middle catchment of the Pecora river, the only significant river entering the basin. The current Pecora river is fully canalized and its discharge into the plain, in the N, is minimal. However, the available

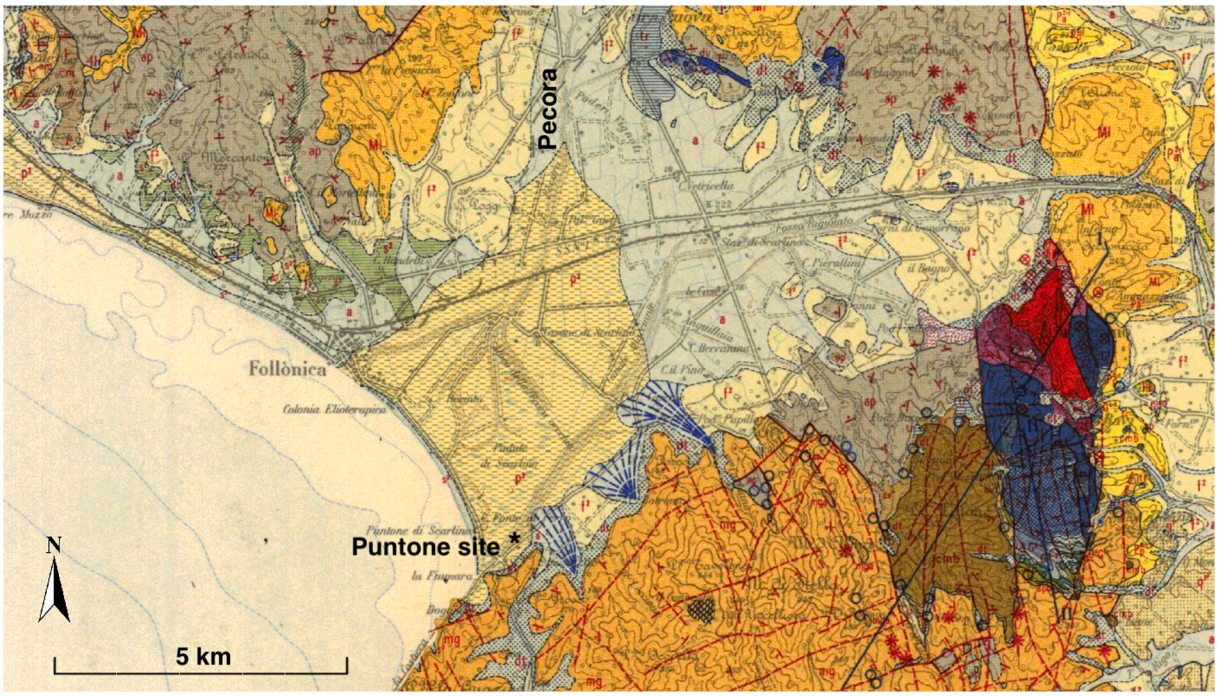

Fig. 2. Geological map of the Follonica coastal basin (From the Carta Geologica d'Italia, 1:100.000, Foglio 127, Piombino). = p^2; = a; = f^2 ; = dt; = alluvial fan; = mg; = ap; = cmb (Early Tertiary carbonatic rocks).

discharge data concern the current situation with large-scale groundwater extraction, and as such they are not relevant for the pre-Industrial period. Coastal currents are weak, some truly limited coastal sand transport taking place from the SW towards Puntone (Aiello et al., 1975). Costantini et al. (2013) published extensive data on the climatic conditions in the Tyrrhenian coastal zone of Central Italy. The annual precipitation is relatively low (ca. 700 mm), and the precipitation deficit is significant (potential evapotranspiration in the order of 1000–1100 mm/year), which at least partly explains the current inland intrusion of seawater along the coastal zone (Positano and Nannucci, 2017). Lastly, the data on calcium (Ca) contents of surficial run-off and groundwater presented by Raco et al. (2015) demonstrated the weak contribution of groundwater from the carbonate rocks (largely originating from the ap formation) to the waters in the southern part of the lagoon, which have the low carbonate signature of the Macigno sandstone, and the alluvial deposits derived from that formation.

3. Material and methods

3.1. Field

The core was taken in the lowest part of the foot slope of the alluvial fan, first to a depth of 115 cm using an Edelman corer, and then with a 6 cm gouge corer from 115 to 325 cm. The rationale for this approach was that the upper 115 cm of the section consisted of very dense, well-aerated non-stratified sediment that clearly was of colluvial origin, emanating from the fan slope above and containing ceramic fragments and charcoal. It was devoid of any marine fauna (shells etc.) and recognisable plant material. Deeper, the same type of sediment was encountered but it was less dense and thus could be sampled with the gouge corer. The composition changed from oxidised to reduced sediment (blueish) at 130 cm depth. Sediments deeper than 320 cm were loamy coarse sands, too incoherent and water saturated to allow undisturbed samples to be taken with a gouge corer.

After obtaining small samples for pollen analysis, the core was sliced into subsamples that were generally 5 cm thick (see Table 1). The subsamples were pretreated with warm 5% KOH (90 °C) and sieved to obtain the fractions >2 mm, 2 mm-150 μm, and 150-63 μm. Material <63 μm was discarded. All material found in the same interval was approximated to be from the same depth, which was taken to be the midpoint depth of that interval.

3.2. Analytical methods

The overall composition of the fractions >150 μm was established using a stereomicroscope. The materials distinguished are listed in Table 1. Terrestrial plant macrofossils (see Table 4) that were suitable for ^{14}C dating were separated by handpicking and subsequent identification under a light microscope. We handpicked fully intact individual *Loripes orbiculatus* shell valves from the fractions >2 mm and subjected single intact valves to a range of analyses, including ^{14}C dating, Sr isotopic composition, and chemical composition. Still hinge-connected valves were only very incidentally encountered, rendering their systematic use impossible. Sediment fractions between 150 and 63 μm were studied microscopically for the presence of 3 components: mica, secondary carbonate, and charcoal, notably to check for the occurrence of tephra and charcoal (potentially representative of human activity). Both fractions were additionally used for identification and quantification of the ostracods. For characteristics and nomenclature of the marine fauna reference is made to www.marinespecies.org.

Pretreatment of all materials for ^{14}C dating was performed at the Centre for Isotope Research (CIO) of the University of Groningen. The single *Loripes* shell valves were first washed with weak (~1%) HCl to remove potential debris embedded in their outer layer, and any recrystallisation that may have occurred to the surface and hence cause the material to date differently from the organism itself (see Dee et al., 2020). The shells were then rinsed well to neutralise the acid, and dissolved in saturated H_3PO_4, releasing the carbonate as $CO_{2(g)}$, which subsequently was reduced to graphite. Plant samples underwent the acid-base-acid (ABA) pretreatment regime used by the CIO (Dee et al., 2020). Each sample was first exposed to HCl (4% vol/vol, 80°CA. 30 min) to remove any surface carbonate. Then, they were rinsed three times with deionised and demineralised water (DW). The next step involved the application of NaOH (1% w/vol, RT, 30 min) to dissolve any humic acids. Once the samples had been rinsed three more times with DW, they were again treated with HCl (4% vol/vol, 80°CA. 30 min), to remove any atmospheric CO_2 absorbed during the alkali step. Finally, they were rinsed again three times with DW, dried and ~5 mg aliquots of the purified product combusted to $CO_{2(g)}$ and then reduced to graphite. The $^{14}C/^{12}C$ ratios of each graphite sample were obtained using the Micadas AMS (Accelerator Mass Spectrometer) instrument at the CIO. The ratios were converted to Fraction Modern values and conventional radiocarbon ages (CRA) using standard procedures. All details of radioisotope measurement, data preparation and uncertainty analysis at CIO are given in Dee et al. (2020) and Aerts-Bijma et al. (2021).

Chemical analysis of the *Loripes* shells were performed on single complete valves that were washed in an ultrasonic bath 2–3 times with Milli Q® H_2O. The shells were crushed, and a small amount (100–250 mg) was dissolved in 1 ml ultrapure HNO_3 (65%) and then diluted to 10 ml using Milli Q® H_2O. In this solution Ca, Mg, Ba, Sr, and B concentrations were estimated using ICP-OES (Inductively Coupled Plasma-Optical Emission Spectroscopy; Optima-8000, PerkinElmer, Waltham, U.S.A.). Aliquots were analysed in triplicate, with the final values representing the respective means.

The Sr isotopic compositions were measured on fragments broken off single complete *Loripes* shell valves. These were first washed in an ultrasonic bath 2–3 times with Milli Q® H_2O, and then washed several times with a mixture of Milli Q® H_2O:H_2O_2 (30–32%) at a ratio of 3:1, to remove any organic material. Once cleaned, samples were dissolved by using ultrapure HNO_3 (65% vol/vol) in closed Savillex® vials. Following dissolution, the acid solution was dried on a hot plate. The solid fractions obtained were redissolved in ultrapure HCl (2.5 M) and centrifuged for 10 min at 5000 rpm. Solutions were then loaded on quartz columns for the chemical separation of Sr by standard Sr isotope geochemistry procedures (Dickin, 2005; Faure, 1986). Samples in duplicate represent shells of different *Loripes* valves on which the isotopic analyses were performed to check the variability in the $^{87}Sr/^{86}Sr$. The selection of the material to analyse was done by excluding fragments of shells and only selecting intact, well-preserved valves of which parts were broken off.

The Sr fractions dissolved in diluted HNO_3 were loaded on degassed Rhenium filaments, to carry out the measurement of $^{87}Sr/^{86}Sr$ isotope ratios by thermal ionisation mass spectrometry (TIMS) at the Radiogenic Isotope Laboratory of the Istituto Nazionale di Geofisica e Vulcanologia (INGV), Osservatorio Vesuviano. Determinations were performed with a ThermoFinnigan Triton TI® multicollector mass spectrometer running in static mode. Measured $^{87}Sr/^{86}Sr$ ratios were normalised for within-run isotopic fractionation to $^{87}Sr/^{86}Sr = 0.1194$. For each measurement, the average 2σ was ±0.000009 (i.e., the standard deviation, $n = 180$). The mean measured value of $^{87}Sr/^{86}Sr$ for the NIST-SRM 987 international standard was 0.710246 ± 0.000019 (2σ, $n = 171$); external reproducibility (2σ) during the period of measurements was calculated according to Deines et al. (2003). The Sr isotope ratios measured were normalised to the recommended value of NIST-SRM 987 ($^{87}Sr/^{86}Sr = 0.71025$). For a full description of the general methods used, reference is made to Arienzo et al. (2013).

For pollen analysis, subsamples of ca. 1 cc were treated with KOH and subsequently acetolysed according to Fægri and Iversen (1989). To separate the organic material from the mineral particles, a bromoform-ethanol mixture (specific gravity = 2) was used. The microfossils were embedded in glycerine jelly and microscope slides were sealed with paraffin. Pollen was identified using Beug (2004), Moore

et al. (1991) and a pollen reference collection. The results are presented in pollen and microfossil diagrams produced with the software TILIA, version 2.0.14.

Where possible, 150 valves of ostracods were counted using a stereomicroscope (Leica EZ4). Species identification was based upon reference papers that were also used for paleoenvironmental interpretations (Athersuch et al., 1989; Henderson, 1990; Mazzini et al., 2017, 2022). The frequency of each taxon was expressed as the number of valves per gram of sediment (raw and dry). Only species represented by both juveniles and adults, or abundant juveniles (more than the 5%) were considered. The use of a 63 μm sieve mesh to process samples allowed the recovery of juvenile and adult valves together with tiny marine taxa balancing the dominating occurrence of the euryhaline species *Cyprideis torosa*, typical of marginal marine environments (Mazzini et al., 2022). The 10 species considered autochthonous were then grouped in OEG (Ostracod ecological/environmental groups) depending on their autoecology (Mazzini et al., 2017). Three groups were identified (see Fig. 3): 1) euryhaline represented by *Cyprideis torosa*; 2) shallow marine represented by *Pontocythere turbida*, *Heterocythereis albomaculata*, *Palmoconcha turbida*, *Aurila arborescens*, *Costa batei*, *Callistocythere* sp.; 3) brackish marine represented by *Xestoleberis dispar*, *Xestoleberis communis*, *Leptocythere ramosa*.

4. Results

4.1. Sedimentary facies and related analyses

The sedimentary sequence encountered in the core is relatively simple and comprises four lithological units and corresponding boundaries (see Table 1, Lithological units).

- At ca. 180 cm depth, from clayey non-stratified sediment of colluvial origin (Unit 1) above this boundary, to clayey sediment with abundant shells that is low in organic matter and with some *Ruppia* (Unit 2, from 180 to 235 cm). The transition from the colluvial material (Unit 1) to the underlying stratified lagoonal sediment (Unit 2) is gradual, the first marine shells being encountered at 176 cm. Remarkably, a large pottery fragment (ca. 5 cm diameter) occurred at 180–184 cm, testifying to an anthropogenic influx to the upper lagoonal strata.
- At ca. 235 cm depth, characterised by a transition from the lagoonal sediment of Unit 2 to fine textured sediment (Unit 3), composed of stratified peaty clay loams and peat containing abundant seagrass material (*Posidonia oceanica*), fruits of *Cymodea nodos*a, and lesser shells, except for its lower section which again is fairly dense with shells (notably *Loripes* and Gastropods). The boundary between Units 2 and 3 is gradual.
- At ca. 325 cm with probably littoral sediment below that depth, given the overall loamy coarse sandy texture and rareness of bivalves (Unit 4).

The lithological units match the faunal zonation, shown in Table 1. Ostracods and foraminifera abound in the 180–235 cm section, while below they are relatively scarce or absent. The bivalves show a more complex pattern: *Loripes* and *Tellinidae/Semelidae* – the dominant species – are prevalent throughout the section below ca. 180 cm, with distinctly lower numbers in the *Posidonia* dominated parts. The same trend is observed for most other bivalves (with overall distinctly lower numbers) and for the gastropods.

General results from the pollen analysis are presented in Table 2 and illustrate the development of the coastal system described above and outlined in Table 1. Pollen concentrations were often very low (of the 17 samples that were studied, 12 had <100 pollen grains, and of these the 5 samples from 250 to 310 cm had <20 grains. A detailed description of these results will be published later. It should be emphasized that the changes in environment/vegetation indicated in Table 2 concern the more regional temporal and spatial development in this part of the Follonica coastal basin. The phases distinguished do not fully comply with the sedimentary units distinguished in Table 1, which are truly site specific, i.e., the coring site and its immediate surroundings.

Data on the ostracods are presented in Fig. 3. They are grouped into three Ostracod Ecological Groups (OEG): Euryhaline, Brackish marine and Shallow marine. Two major boundaries exist: one at 290 cm, below which shallow and brackish marine species represent the dominant groups, and one at 230 cm, above which the euryhaline species (*Cyprideis torosa*) rapidly increased to become by far the dominant species. A diversified assemblage of shallow and brackish marine species was only truly encountered in the samples from 305 to 295 cm (*Pontocythere turbida, Heterocythereis albomaculata, Palmoconcha turbida, Costa atei, Callistocythere* sp., *Xestoleberis dispar*, *Xestoleberis communis*, *Leptocythere ramosa)*. At 216 cm, the well-preserved shallow marine species *Aurila arborescens* occurred within a *C. torosa* dominated assemblage.

The chemical composition of the *Loripes* shells is shown in Table 3. For the upper part of the core, none of these shells were found and thus no data were produced. The materials analysed are from the sedimentary units 2 and 3 described above: 192–235 cm (shell-rich sediment) and 235–325 cm (seagrass dominated sediment). Mean values for each of these units are indicated, excluding the transitional sediment stratum (230–237.5 cm). Ca and Sr contents are relatively constant, while differences exist in the mean values for Ba and Mg, and in the mean Ba/Ca and Mg/Ca ratios. However, differences between the two units (192–230 cm and 237.5–317 cm) were only significant for Mg concentrations and Mg/Ca ratios (ANOVA test, $p = 0.005$ for Mg and $p = 0.004$ for Mg/Ca ratios).

Data on the Sr isotopic composition of the *Loripes* shells are presented in Table 3 and Fig. 4. Given the analytical error ($\sigma = 0.000019$) we calculated the mean value of $^{87}Sr/^{86}Sr$ for shells from depths from 192 to 270 cm. The mean Sr isotopic composition is 0.70910 ($\sigma = 0.00001$), including those for duplicate/triplicate estimations. Samples from 295 to 317 cm have highest values (ca. 0.70914), nearing those for seawater and those for the shells found earlier in the processed sediment from the *briquetage* site at Puntone (green box in Fig. 4; data in Sevink et al. (2021).

4.2. Radiocarbon calibration and age-depth Bayesian modelling

The results of the ^{14}C analyses are presented in Tables 4 and 5. In all, 13 dates were obtained on the terrestrial plant samples, across a range of taxa, as is shown in Table 4. Unfortunately, because of the diminutive size of the plant samples, these data are frequently accompanied by much larger uncertainties than would normally be the case. The raw results were calibrated against IntCal20 (Reimer et al., 2020) revealing the absolute age of the sedimentary sequence across its entire extent. To refine the absolute date ranges, an age-depth model was built in the Bayesian chronological modelling program OxCal (Ramsey, 1995); however, as shown in Fig. 5a, only limited gains in precision were achievable in this case, particularly for the more recent samples. Moreover, three samples (GrM-29925, 28181 and 27797) were determined by the program's outlier function to be inconsistent with the series as a whole. For the modelled sequence, however, mean absolute dates (in year cal BP) were extractable from the outputs as best approximations for the true age of that layer.

A total of 15 results were obtained on the marine shells (Table 5). These were calibrated against Marine20 (Heaton et al., 2020). As they were larger samples, they generated more precise results, and returned a compelling age-depth profile, as shown in Fig. 5b. Indeed, only one, GrM-27744, was deemed by OxCal to be an outlier, and was excluded from the rest of the analysis. The OxCal code for both the terrestrial and marine models is given in the Appendix.

Outliers in the radiocarbon dating of environmental contexts can

Table 1
Composition of the fractions 150-63 μm (mineral) and the fractions >150 μm.

Lithol. units	Depth in cm	Fraction >150 μm														
		Mica	Secondary carbonate	Charcoal	Materials other than mollusks											
					Roots	Seeds and other	Charcoal	Ceramic	Hard	Gravel	Ostracoda	Foramin.	Spirorbis	Astro-	Echinoidea	Crustacea
					Posidonia	plant remains		material	clay ball	>2 mm			sp.	pecten		
					oceanica	+ number								sp.		
Unit 1	150–154	tr	tr		–	Rubus-1, cf Mentha-1	x	–	x	1	–	–	–	–	–	–
	154–157	tr	x	x	–	–	–	–	–	–	–	–	–	–	–	–
	157–161	tr	x	tr	–	–	–	–	x	–	–	–	–	–	–	–
	161–168	(x)	(x)	(x)	–	–	1	–	x	–	–	–	–	–	–	–
	168–173	(x)	(x)	(x)	x	–	x	? 1 cm	–	–	–	–	–	–	–	–
	173–176	tr	tr	tr	x	Vitis-1	x	–	–	–	–	–	–	–	–	–
	176–180	x	x	x	x	Vitis-1 fr., Juncus-1	x	–	–	1	xx	x	–	–	–	–
Unit 2	180–184	tr	x	tr	x	–	x	5 cm	1	2	xxxx	x	–	–	–	–
	184–188	x	x	x	–	Ruppia-1	x	–	–	–	xxxx	xx	–	–	–	–
	188–192	x	xx	xx	–	–	x	–	–	–	xxxx	xxx	1	–	–	–
	192–196		xx	x	x	Ruppia-2	x	–	–	–	xxxx	–	–	–	–	–
	196–200		xx	x	–	–	–	–	–	–	xxxx	x	–	–	–	–
	200–204		xx	x	x	Ruppia-1	–	–	–	–	xxxx	x	–	–	–	–
	204–208		xx		x	–	–	–	–	–	xxxx	xx	–	–	–	–
	208–212		x	x	x	Ruppia-1	–	–	–	1	xxxx	xx	–	–	–	–
	212–216		x	x	–	–	–	–	–	–	xxxx	xxx	–	–	–	–
	216–220	tr	x	(x)	xx	Juncus-1	–	–	–	x	xxxx	xxx	–	–	–	–
	220–221	tr	x	(x)	x	–	–	–	–	–	xxx	xx	–	–	–	–
	221–222				x	Ruppia-2	–	–	–	–	xxx	xx	–	–	–	–
	222–223				x	–	–	–	–	–	xxx	xx	–	–	–	–
	223-227,5		x	x	xx	? - 1 fr.	1	–	–	–	xxxx	xx	1	–	–	–
	227,5-230	(x)	x	(x)	x	–	–	–	–	1	xxx	x	–	–	–	–
	230–235	(x)	x	(x)	x	–	x	–	–	1	xxx	xxx	–	–	–	–
Unit 3	235-237,5	(x)	(x)	(x)	xxxx	leaf (charcoal)		–	–	–	x	x	–	–	–	–
	237,5-240	(x)	(x)	(x)	xxxx	–	–	–	–	–	x	x	–	–	–	–
	240–245	x	x	(x)	xxxx	–	–	–	–	–	x	x	–	–	–	–
	245–252	x	x	x	xxxx	–	–	–	–	–	x	x	–	–	–	–
	252–260	tr	tr	(x)	xxxx	–	–	–	–	–	–	x	–	–	–	–
	260–265	x	x	x	xxxx	–	–	–	–	–	x	x	–	–	–	–
	265–270	tr	tr		xxxx	Cornus mas-1 fr., ?-1	–	–	–	–	–	–	–	–	–	–
	270–275	x	x	x	xxxx	Quercus sp.-x fr., ?-1	–	–	–	–	–	–	–	–	–	–
	275–280	tr	tr	(x)	xxxx	? - 2	xx	–	–	–	–	–	–	–	–	–
	280–285	x	(x)	x	xxxx	–	–	–	–	–	–	–	–	–	–	–
	285–290	x	(x)	x	xxxx	–	–	–	–	–	–	–	–	–	–	–
	290–295	x	(tr)	(x)	xxxx	–	–	–	–	–	–	–	–	–	–	–
	295–300	(x)	(x)	(x)	xxxx	Rubus sp.-2 fr., Cornus mas-1	xx	–	–	x	x	x	3	–	–	1 fr.
	300–305	tr	(x)	(x)	xxxx	x *	xx	–	–	x	x	x	–	1 fr.	3 fr.	–
	305–310	(x)	(x)	(x)	xxxx	Rubus sp.-2, Verbena-1	x	–	–	x	x	x	1	–	–	–
	310–317	tr	tr		xxxx	moss-1, Posidonia	x	–	–	x	x	x	1	cf 1 fr.	–	–
	317–325	(x)	(x)	(x)	xxxx	Posidonia ?	–	–	–	–	–	x	1	1 fr.	–	–

Legend fraction 150-63 μm: tr = trace; (x) = some; x = common; xx = many.
Legend fraction >150 μm: x = some; xx = tens; xxx = hundreds; xxxx = thousands (or >); fr. = fragment.
x* = Rubus sp.-3, Fumaria-2, Polygonum aviculare-1, moss-2 fr, Posidonia ?
Analysis: W.J. Kuijper, April 2021.

Bivalves								Gastropods						
Loripes orbiculatus	Cardiidae	Acantho-cardium tuberc.	Cerasto-derma glaucum	Tellinidae, Semelidae	Veneridae	Ostrea ?	Mytilidae	Bittium reticulatum	Cerithium vulgatum	Cerithiidae Cerithiopsidae Potamididae	Hydrobia sp. (c. 3 sp.)	Rissoa ? Gibbula ?	Tritia neritea	Retusa cf trunc.
–	–	–	–	–	–	–	–	–	–	–	–	–	–	–
–	–	–	–	–	–	–	–	–	–	–	–	–	–	–
–	–	–	–	–	–	–	–	–	–	–	–	–	–	–
–	–	–	–	–	–	–	–	–	–	–	–	–	–	–
–	–	–	–	–	–	–	–	–	–	–	–	–	–	–
–	–	–	–	–	–	–	–	–	–	–	–	–	–	–
–	x fr.	–	–	x fr.	–	–	–	1	x fr.	–	xx	–	–	–
x fr.	x	–	x ?	x fr.	–	–	–	–	1	x	xx	Rissoa - 1 fr.	–	–
x fr.	–	–	x ?	x fr.	–	–	–	1 ?	–	x	xxx	–	–	–
1, xxfr.	–	–	1, x fr.	x fr.	–	–	–	1, 1 fr.	–	–	xxx	–	–	–
x	–	–	x, x fr.	xx fr.	–	–	–	x	x, xx fr.	–	xxx	Rissoa sp.-1	3	1
x, xx fr.	–	–	x, x fr.	xx fr.	–	–	–	x	x, x fr.	–	xxxx	–	4	2
x, xx fr.	1, x fr	–	1, xx fr.	x, x fr.	–	–	–	x	x	x, x fr.	xxxx	–	4	1
x, xx fr.	–	–	1, x fr.	x, xx fr.	–	–	–	x	x, x fr.	–	xxxx	–	2, 3 fr.	2, 1 fr.
xx	x	–	–	xx fr.	1 fr.	–	–	x	x	x fr.	xxx	–	8	2
x, xx fr.	–	–	x fr.	x fr.	–	–	–	xx	x, x fr.	–	xxxx	–	1, 3 fr.	1
x, x fr.	x fr.	–	–	x fr.	–	–	–	x	1	–	xxx	–	1 fr.	–
x, x fr.	1, x fr.	1	–	1, x fr.	–	–	–	x	2	–	xxx	–	2 fr.	1
x, x fr.	x fr.	–	–	x fr.	–	–	–	x	1	–	xxx	–	3 fr.	–
x, xx fr.	x fr.	–	1, x fr.	xx fr.	–	–	–	x	x. x fr.	–	xxxx	Rissoa - 2	x, x fr.	x
x, xx fr.	x fr.	–	1, x fr.	xx fr.	x ?	–	–	xx	3, xx fr.	–	xxx	–	3, x fr.	1, 2 fr.
x, xx fr.	1, x fr.	1	–	x, xx fr.	–	–	1 fr.	xx	x, xx fr.	–	xxxx	–	3, 2 fr.	2, 2 fr.
x, xx fr.	x fr.	–	–	x fr.	–	–	–	x, x fr.	1, x fr.	–	xx	–	2 fr.	1
xx fr.	1 fr.	–	–	x fr.	–	–	–	xx	1, 1 fr.	–	xx	–	2	–
x, xx fr.	–	–	–	x	–	–	–	xx	x, x fr.	–	xx	–	5	–
xx	–	–	1 fr.	x fr.	cf xx fr.	–	–	xx	1, x fr.	–	xxx	–	6	–
xx	–	–	x fr.	–	x fr.	–	–	xx	x	–	xxx	Rissoa-1	8	–
xx	–	–	1, x fr.	x	–	–	–	xx	x, x fr.	–	xxx	–	7	–
x, x fr.	–	–	2 fr.	–	–	–	–	x	1 fr.	–	xx	–	–	–
x fr.	1 fr.	–	–	–	–	–	–	1	–	–	x	–	–	–
–	–	–	–	2 fr.	–	–	–	–	–	–	–	cf Gibbula-1	–	–
–	–	–	–	–	–	–	–	–	–	–	–	–	–	–
–	–	–	–	–	–	–	–	–	–	–	–	–	–	–
–	–	–	–	–	–	–	–	–	–	–	–	–	–	–
xx	–	–	1, 2 fr.	x, x fr.	1, 1 fr.	–	2 fr.	xx	x	–	xx	–	1	3
xx	1 fr.	–	3 fr. cf	xx fr.	2, 1 fr.	3 fr.[= 1]	–	xx	1 fr.	–	xx	–	–	1
xx	–	1 fr.	3 fr.	x, x fr.	1 fr.	–	1 fr.	xxx	2, 1 fr.	–	xx	Odostomia-1	–	1
xx	–	–	–	x. x fr.	1, 1 fr.	1 fr.	1	xxx	x fr.	–	xx	?	2	1
1, x fr.	–	–	x fr.	xx	–	–	–	xx	1 fr.	–	x	–	1 fr.	–

arise from a multitude of causes. Marine shells in sedimentary cores are usually too large to be easily reworked, but the material is durable, so such displacement is always a possibility. More common are offsets to younger due to recrystallisation of the carbonate matrix by more recently dissolved bicarbonate. Terrestrial plant samples by definition have been transported into the sea and are hence often more fragmentary and potentially mobile, especially via bioturbation, in the sediment, resulting in younger outliers. An extensive literature exists on bioturbation in shallow coastal environments, notably in mangroves and mudflats (e.g., Teal et al., 2008; Booth et al., 2023). There is a vast range of burrowing benthic species, amongst which the lucinid species that we studied, and all studies on bioturbation stress the important role of bioturbation in such sediments. In a dynamic, natural environment it is almost impossible to avoid outlying results, and this is even before any potential contribution from contamination during handling and laboratory pretreatment. Considering this, the general congruence of both our models with depth is reassuring.

Superimposing the outputs of the plant and shell age-depth models would not provide information on the temporal variation of the MRE. As described above, ΔR is defined as the difference between *uncalibrated* ^{14}C results obtained on marine samples and the Marine20 calibration curve at any given moment in time. Nonetheless, several methods exist for estimation of the diachronic profile of the MRE, two of which are applied here. In the first, ΔR is derived from the uncalibrated ^{14}C data obtained on paired samples (terrestrial and marine materials from the same depth). Reimer and Reimer (2017) provide an online tool called *deltar* for this scenario. In this case, the ΔR values calculated are taken to pertain to the midpoint of the calibrated probability density function of the terrestrial sample. Table 6 indicates the pairs of samples from our study for which these exact offsets can be determined. The terrestrial samples, from the depth of 273 cm (GrM-30063 & GrM-27798) are automatically averaged by OxCal's age-depth modelling algorithm, as the program assumes they come from the same year. However, they are independent samples and do not pass the χ^2-test when averaged. For this reason, their ΔR values are calculated separately in the *deltar* program.

ΔR can also be estimated by producing a plot of uncalibrated age versus absolute time for the marine samples and calculating its divergence from Marine20. To do this, as with *deltar*, the median values of the modelled dates from the terrestrial age-depth model are used to assign absolute ages to each depth in the core. Given the imprecision of our plant results, this is a somewhat crude approach, but no other method was clearly more satisfactory. The 12 marine results which were available at depths where the plant and marine sequences overlap (190–302.5 cm) or 303 cm (see Table 4) were then assigned absolute ages using this terrestrial age-depth relationship (excluding one outlier, GrM-27744, mentioned above). For these 12 points, the difference between the uncalibrated ^{14}C value and Marine20 (i.e., ΔR) could then be estimated. Here the uncertainty in ΔR is taken to be the quadratic sum of the uncertainty in each of our results and Marine20 for that year. To produce a continuous representation of our uncalibrated terrestrial, marine and ΔR values against absolute time (Fig. 6a and b), a polynomial interpolation (degree = 4) is passed through the data sets and their ±1σ values in *python*.

5. Discussion

5.1. Loripes orbiculatus and the marine reservoir effect (MRE)

Loripes orbiculatus is a benthic marine mollusc from the family *Lucinidae* that lives in shallow marine environments, notably in seagrass fields (Honkoop et al., 2008; Cardini et al., 2022). It is a symbiotic species harbouring endo-cellular sulphur-oxidizing bacteria within its gills, burrowing into sediment, and living at the boundary between oxic and anoxic sediment, with inhalant/exhalant tubes lined with mucus (e.g., Yuen et al., 2019; Zauner et al., 2022). The burrow depth is equal to the length of its extended foot (Allen, 1953, 1958; Taylor and Glover,

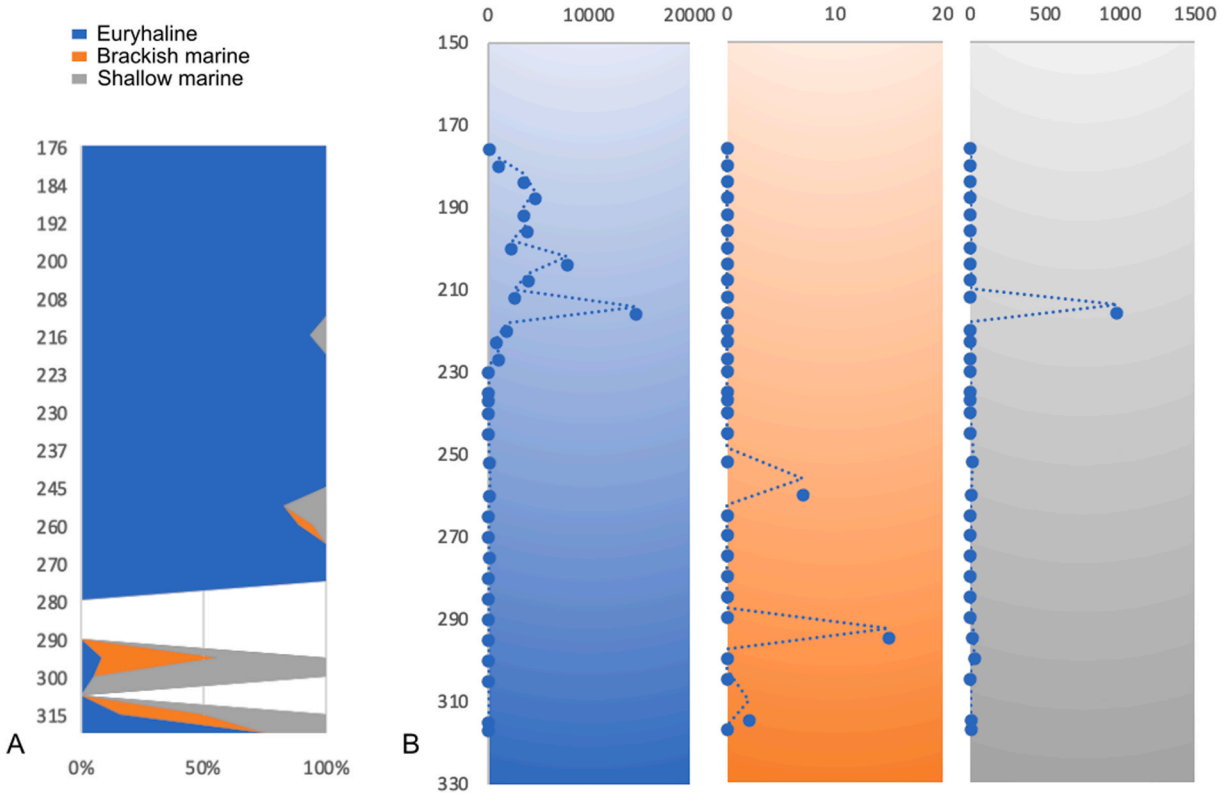

Fig. 3. Ostracod data: A) 100% stacked area chart of the 3 Ostracod Ecological Groups where each group is shown as a proportion of the whole instead of numerical values. B) Normalised frequencies of the 3 OEG. Basic data is provided in appendix 3.

Table 2
Results from the pollen analysis in terms of the vegetation types encountered.

Depth in cm	Vegetation	Indicator species	Remarks
150–140	Salt marsh	*Aster tripolium*	Established high salt marsh vegetation
190–150	Lagoonal	*Ruppia maritima*	Increase in Atriplex type pollen, start higher salt marsh vegetation
230–190	Lagoonal	*Ruppia maritima*	Submerged species, aquatic conditions
250–230	Salt marsh	*Limonium*	Start of salt marsh formation
280–250	Marine	Seagrasses	Low pollen count, some macroremains
325–280	Marine	Driftmark litter	

2000, 2006; van der Geest et al., 2011). A resulting complication is that an in-situ shell of this mollusc postdates the layer of sediment into which it has burrowed.

To avoid a potential error in the assessment of the MRE caused by reworking of older shell material, we obtained ^{14}C ages for complete shells valves that were handpicked from the various fractions. This, however, leaves burrowing as another potential source of error, the magnitude of which can be approximated from the sedimentation rate obtained from the radiocarbon data (see also 4.2). The likely maximum age offsets between the *Loripes* shells and their surrounding sediment, based on mean burrowing depths of 5 and 10 cm, are 15–35 years for sediment unit 3, and 125–250 years for unit 2. The uncertainty in such estimates is patently significant, given the mean thickness of the samples is only 5 cm. But the key implication is that ΔR values for unit 3 are likely to be close to their 'true' values, whereas the 'true' ΔR values for shells from unit 2, may be significantly higher.

Another important consideration is that sugars produced by the symbionts are an important source of food for the *Loripes* molluscs, in addition to organic material taken in from the seawater (e.g., Roques et al., 2020). Carbon dioxide required by the bacterial symbionts is provided by the mollusc but its source remains rather uncertain. It is both described as being absorbed by the mollusc from pore water in the adjacent sediment (e.g., Van der Heide et al., 2012; Stanley, 2014) and elsewhere as originating from the inhaled seawater via carbonic anhydrases of HCO_3^- (e.g., Rossi et al., 2013; Yuen et al., 2019). CO_2/HCO_3^- in pore water may originate from anaerobic microbial decomposition of pre-existing material in the sediment column and thus would potentially lead to an increase in the age offset of the organism and the sediment, and hence of the MRE. A typical example of such a process is diagenetic methanogenesis, which is accompanied by carbon dioxide production (see e.g., Whiticar, 2002; Jilbert et al., 2021)

Alves et al. (2018) published a thorough review of the MRE, and the complex carbon cycle that controls this effect. Further, Lindauer et al. (2022) gave an extensive overview of the difficulties encountered when using molluscs for ^{14}C dating, paying particular attention to the sources of the carbon built into biogenic carbonate structures. In both studies examples were given of significant temporal variation in the ^{14}C concentration of the reservoirs utilised by different organisms.

Our results indicate that during the deposition of unit 3 the magnitude of the ΔR based on the Loripes data is typical of what is used for marine calibration; although the only two results from the northern Tyrrhenian Sea in the CHRONO database average to a slightly lower -149 ± 42 ^{14}C yr (Taviani & Correggiari, pers comms). However, during unit 2 the ΔR value strongly increases. The only plausible explanation is a significant decrease in the ^{14}C content of the carbon taken up and fixed in their shell by the *Loripes* molluscs. The relevant sources comprise dissolved carbon dioxide ($CO_{2(aq)}$), bicarbonate (HCO_3^-), carbonate (CO_3^{2-}) and organic carbon from sea water ingested by *L. orbiculatus* through its inhalant tube or absorbed from pore water in the sediment column. Of these, the principal two are expected to be HCO_3^- and organic carbon (food) (see e.g., Williams and Follows, 2011; Zeebe, 2012). The molluscs deliver inorganic carbon to their symbiotic bacteria, which return carbohydrates (sugar) to their host. This exchange forms a significant, but variable component of the total food ingested by the mollusc (e.g., Roques et al., 2020). The question thus arises whether this temporal variation in the ΔR can be linked to the changes in environment/facies that occurred during the period concerned, which may have led to variation in the ^{14}C content of these

Table 3
Chemical and Sr-isotopic composition of the *Loripes* shells. from lithological units 2(upper) and 3 (lower).

Sample with depth in cm	Ca (mg/g)	Sr (mg/g)	B (μg/g)	Ba (μg/g)	Mg (μg/g)	Ba/Ca μg/mg*103	Sr/Ca mg/mg*103	Mg/Ca μg/mg*103	B/Ca μg/mg*103	87Sr/86Sr ratios		
Loripes										shell	replicate 1	replicate 2
PU 192-196	367	1.64	25.7	2.88	174	7.8	4.47	0.47	70	0.709107	0.709098	n.d.
PU 196-200	369	1.72	20.3	1.18	213	3.2	4.66	0.58	55	0.709086	0.709094	0.70909
PU 200-204	362	1.83	12.6	2.90	237	8.0	5.06	0.65	35	0.709111	0.709099	n.d.
PU 204-208	371	1.82	12.9	3.07	213	8.3	4.91	0.57	35	0.709097	n.d.	n.d.
PU 208-212	361	1.84	19.2	3.70	178	10.2	5.10	0.49	53	0.709094	n.d.	n.d.
PU 212-216	356	1.73	15.3	3.21	159	9.0	4.86	0.45	43	0.709098	n.d.	n.d.
PU 216-220	367	1.75	13.3	2.03	223	5.5	4.77	0.61	36	0.709106	0.709104	n.d.
PU 220-223	376	1.65	16.1	3.09	214	8.2	4.39	0.57	43	0.709098	n.d.	n.d.
PU 223-227	358	1.72	14.1	1.28	212	3.6	4.80	0.59	39	0.709112	n.d.	n.d.
PU 227-230	362	1.87	12.6	1.96	213	5.4	5.17	0.59	35	0.709082	0.709095	n.d.
PU 230-235	332	1.67	12.9	2.00	242	6.0	5.03	0.73	39	0.709086	0.709085	0.70908
Mean	**365**	**1.76**	**16.2**	**2.53**	**204**	**6.9**	**4.82**	**0.56**	**44**			
PU 235–237.5	366	1.83	20.4	7.20	160	19.7	5.00	0.44	56	0.709113	n.d.	n.d.
PU 237.5–240	366	1.78	15.4	2.25	142	6.1	4.86	0.39	42	0.709103	n.d.	n.d.
PU 240-245	346	1.68	13.2	2.02	196	5.8	4.86	0.57	38	0.709109	0.709121	n.d.
PU 245-252	364	1.76	11.6	2.25	152	6.2	4.84	0.42	32	0.709093	n.d.	n.d.
PU 252-260	375	1.85	19.0	2.00	184	5.3	4.93	0.49	51	0.709080	n.d.	n.d.
PU 260-265	362	1.81	15.1	2.52	187	7.0	5.00	0.52	42	0.709083	0.709070	n.d.
PU 265-270	359	1.82	13.8	3.17	187	8.8	5.07	0.52	38	0.709104	0.70910	n.d.
PU 295-300	337	1.54	12.7	3.00	152	8.9	4.57	0.45	38	0.709124	0.709130	n.d.
PU 300-305	368	1.64	19.8	5.05	138	13.7	4.46	0.38	54	n.d.	n.d.	n.d.
PU 305-310	368	1.60	24.3	3.11	176	8.5	4.35	0.48	66	0.709133	0.70915	n.d.
PU 310-317	364	1.80	14.4	3.81	158	10.5	4.95	0.43	40	0.709145	0.709146	n.d.
Mean	**361**	**1.73**	**15.9**	**2.92**	**167**	**8.1**	**4.79**	**0.46**	**44**			
P value	*0.955*	*0.598*	*0.881*	*0.298*	*0.005*	*0.313*	*0.793*	*0.004*	*0.935*			

Table 4
The ^{14}C results obtained on the terrestrial plant samples from Puntone. The absolute date ranges from the OxCal age-depth model (against IntCal20) are also given.

Terrestrial Plants													
Lab Ref		Sample Detail	Depth (cm)			d13C (‰, VPDB)[c]	14C Age		Modelled Date (IntCal20, Year cal BP)				
			Top	Bottom	Average		14C yr BP	±1σ	From (68%)	To (68%)	From (95%)	To (95%)	Mean
	GrM-28182	Charred Erica leaf	150	154	152	–	2080	140	2355	1737	2461	1624	2107
	GrM-28183	Charred Erica leaf	157	161	159	–	2520	100	2503	1768	2570	1705	2217
	GrM-27795	Waterlogged Vitis fruit	173	176	175	−28.09	1927	22	2603	1832	2665	1821	2323
	GrM-27893	Charred Erica leaf	184	188	186	–	2370	35	2669	2345	2697	2332	2483
	GrM-29925	*waterlogged Vitis fruit*	*192*	*196*	*194*	-	*2190*	*110*	*2720*	*2397*	*2798*	*2343*	*2580*
	GrM-28184	Charred Erica leaf	200	201	201	–	2670	110	2920	2623	2993	2490	2765
a	GrM-29926	Charred Erica leaf	212	216	214	–	2980	110	3232	2964	3360	2873	3113
	GrM-29927	Waterlogged Medicago perianth	235	238	236	–	3460	110	3696	3469	3803	3389	3583
	GrM-28181	*Waterlogged Rubus fruit*	*245*	*252*	*249*	-	*2330*	*100*	*3828*	*3618*	*3881*	*3494*	*3696*
a	GrM-30060	Waterlogged Oak cupula	260	265	263	−27.39	3641	26	3910	3839	3945	3680	3844
	GrM-27797	*Waterlogged Medicago fruit*	*265*	*270*	*268*	*−25.34*	*4034*	*26*	*3914*	*3843*	*3953*	*3722*	*3861*
b	GrM-30063	Waterlogges Oak cupula	270	275	273	−23.20	3495	24	3921	3846	3959	3731	3876
b	GrM-27798	Waterlogged Cornus mas endocarp	270	275	273	−24.88	3650	26					
	GrM-30064	Waterlogged Oak cupula	275	275	275	–	3683	26	3941	3847	3962	3734	3887
	GrM-27799	Waterlogged Rosaceae thorn	285	290	288	−25.98	3554	26	3962	3862	3973	3832	3909
a	GrM-27800	Waterlogged Rubus fruit	300	305	303	−26.62	3549	26	3974	3873	4087	3860	3951

[a] Paired with marine samples.
[b] Results from same average depth are automatically averaged by OxCal, but statistically speaking they should not be.
[c] Samples measured directly using gas-ion AMS interface could not have d13C measured on IRMS.

carbon sources.

5.2. Diachronic changes in sedimentary environment

Based on the palaeoecological data (fauna and flora) successive sedimentary units were distinguished for which sedimentation rates could be established. This sequence evidently can be placed in the context of Holocene sea level rise. The earliest marine sediments encountered in the core (below 325 cm) likely reflect the local onset of the Holocene transgression around 2500 BCE (ca. 4550 cal BP). A marine seagrass ecosystem developed with its characteristic fauna and the highest sedimentation rate of the whole sequence studied (ca. 3 mm/year). Whether this was in a shallow bay or open lagoon is not clear, but the faunal and floral data point toward a distinctly marine environment. Around 1700 BCE (3650 cal BP) at ca. 230 cm depth) the seagrasses declined, and a shallow lagoon developed with a far sparser marine vegetation. It is very likely that at that stage a beach ridge had formed, protecting the lagoon against serious wave action and the accrual of coarse (sand-sized) clastic material by long-shore currents (Aiello et al., 1975). However, the lagoon remained in open connection with the sea until very recently. The connection with the sea is testified by the abundant *Posidonia oceanica* remains and fruits of *Cymodea nodosa*, and by the appearance of *A. arborescens* at 216 cm. *A. arborescens* is typical of very shallow vegetated marine habitats, with sandy bottoms. At this point, the sedimentation rate sharply declined to ca. 0.4 mm/year and marine fauna became more abundant, notably ostracods and foraminifera. By the end of this period, around 400 BCE (ca. 2350 cal BP), a lagoonal saltmarsh-type of ecosystem had developed, and sea level had reached its current level (Lambeck et al., 2004).

During the early period (unit 3), characterised by a marine seagrass ecosystem in a shallow bay or open lagoon, the water chemistry and salinity must have been that of open sea. Given the relatively dry climate of the Tuscan coastal area (ca. 700 mm annual precipitation) and a significant precipitation deficit in this specific area (e.g., Positano and Nannucci, 2017), in an enclosed lagoon and particularly during the saltmarsh phase (unit 2) the salinity must have increased, unless the evaporation losses were balanced by an influx of terrestrial run-off, river water or groundwater. Regarding such influx, detailed studies on the geohydrology of the Follonica basin (e.g., Masetti et al., 2017) show that it was, and remains, rather meagre due to the limited size of the catchment feeding the lagoon (mainly the Pecora River) and the very low hydraulic conductivity of the Quaternary sedimentary fill of the basin, which strongly reduces any groundwater flow from the hinterland. Currently, the coastal area is even marked by seawater intrusion, but this is largely attributed to the inland groundwater extraction (Positano and Nannucci, 2017). Lastly, the low sedimentation rate is also consistent with a very low level of inflow from terrestrial waters and their associated sediment.

Clear indications for increasing salinity during the deposition of unit 2 were found in the ostracod and pollen analyses. The ostracod *C. torosa* can dominate benthic communities of saline water bodies, sometimes reaching extremely large abundances (Heip, 1976). *C. torosa* reaches high populations in biotopes with considerable salinity fluctuations, and its upper limit of salinity tolerance reaches 96–150 g l-1 (Bodergat et al., 1991; De Deckker and Lord, 2017). The change in facies also coincided with an increase in Mg content of the *Loripes* shells, while their Mg/Ca

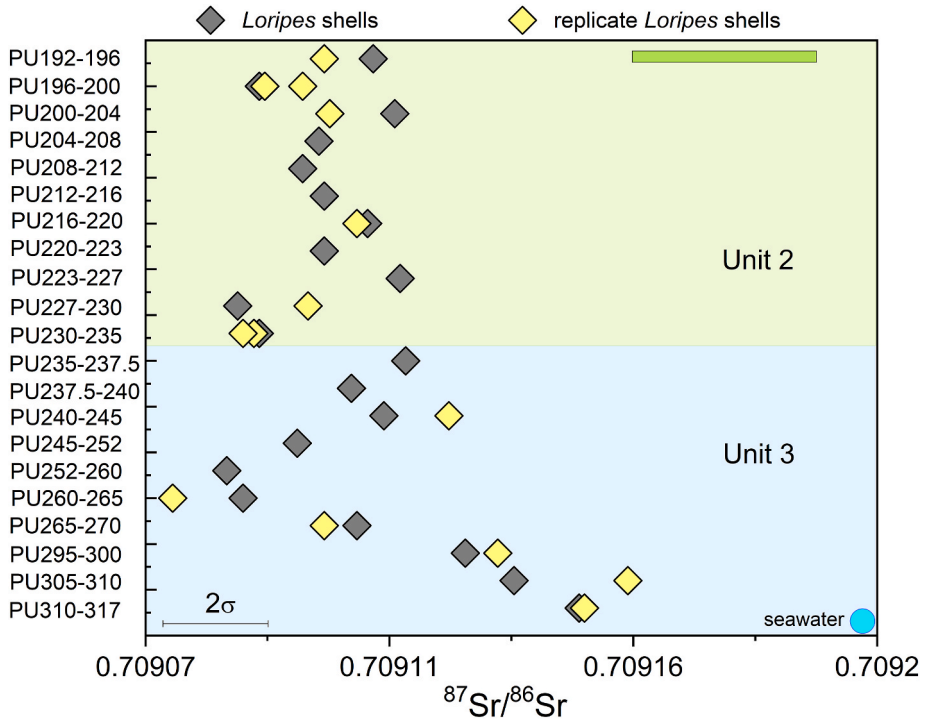

Fig. 4. Sr isotopic composition of the *Loripes* shells. The range in ratios found for shells in earlier studies (Sevink et al., 2020, 2021) is indicated with a green bar; the ratio for seawater from the Tyrrhenian Sea with a blue dot.

ratios also increased. This might point to higher overall water temperature and/or increased salinity (Butler et al., 2015; Poulain et al., 2015), which would also accord with the development of a shallower and more enclosed, more saline lagoon. However, the use of these elemental proxies for identification of environmental conditions are still fraught with problems (Immenhauser et al., 2016).

Potentially relevant information is also provided by the Sr isotopic analyses of the *Loripes* shells, since they may also reflect changes in the salinity due to admixture with water of different isotopic ratio than seawater. Such waters may have varied $^{87}Sr/^{86}Sr$ ratios, being dependent on the characteristics of the sediments in the drainage basin from which they originate, notably of the isotopic ratios of carbonates present in these sediments, which are highly soluble relative to silicate minerals. As already shown by Sevink et al. (2021), run-off and groundwater flow from the hills to the south of the Follonica basin very likely had much higher Sr isotopic ratios than seawater, as the deeply decalcified soils and sediments in these catchments are derived from the Macigno Formation which is known to have such high Sr isotopic ratios (ca. 0.7155; Boschetti et al., 2005; Nisi et al., 2008). The available isotopic data on river discharge, notably of the nearby Cornia River, the main contributor to the Gulf of Follonica, also show a significant river discharge characterized by a distinctly higher Sr isotopic ratio than that of seawater (Pennisi et al., 2009).

Fig. 4 demonstrates that Sr isotopic ratios of the lowermost samples are closer to those of seawater than those above, which are ostensibly rather variable. Lowest values are encountered at 260–265 cm, but the apparent trend cannot be linked to a specific change in sedimentary facies, which for unit 3 is distinctly marine throughout. Moreover, the analytical error for shells from depths of 192–270 cm is such that the differences are not significant and all fall within a common range for coastal waters. An alternative might be a slight fractionation of Sr isotopes in biogenic carbonates, which would be temperature and salinity dependent (Shao et al., 2021) and, eventually, a slight difference in such fractionation between benthic mud-dwelling molluscs and pelagic mollucs for which data were presented by Sevink (2020, 2021). Yet, strontium isotopic applications are described as 'in their infancy' by Liu et al. (2015) and fractionation was not observed in their experimental study, nor in other studies on Sr isotopic ratios in molluscs.

Lastly, circumstantial evidence for a relatively high salinity of the shallow lagoonal/salt marsh ecosystems was already presented by Sevink et al. (2020, 2021), who studied prehistoric salt production by *briquetage* at Puntone, which was based on leaching of sediment taken from the lagoonal area during phase 2. They concluded that in the upper sediment layer evaporation and the resulting increased salinity reached a level at which carbonate precipitated, which takes place at a brine concentration of about 1.8 times that of seawater (McCaffrey et al., 1987).

5.3. Causes of the observed variability of the MRE values

High ΔR values are generally linked with such phenomena as an increased input of 'old' terrestrial carbon in the form of organic carbon or bicarbonate (e.g., Quarta et al., 2021, for the Mar Piccolo Sea basin in Taranto, southern Italy), upwelling of older ocean waters (e.g., Alves et al., 2018; Lindauer et al., 2022), and an intake of old carbonate (detrital carbonatic rock) by benthic molluscs (e.g., Petchey et al., 2012).

From the discussion in 5.2 it is evident that there is no indication for an increased input of such older terrestrial carbon upon the change in environmental conditions in the Puntone area i.e., for a hard water effect. Given the very limited river and groundwater discharge and low calcium carbonate content of the rocks and groundwater in the area concerned, for a shallow lagoonal environment open to the sea such an increase in old carbon is highly improbable. Moreover, the chemical data on the *Loripes* shells discussed above, particularly the Sr isotopic data, argue against an increase in terrestrial input. As to an increase in the upwelling of older seawater, such a phenomenon is highly improbable to have occurred during the passage from an open, but shallow bay to a semi-closed lagoon in this Mediterranean coastal basin with its weak currents.

There is no reason to assume that incidental uptake of old carbonate (detrital carbonatic rock) by *Loripes* would be relevant for our study

Table 5
The ^{14}C results and △R values obtained on the marine shell samples from Puntone. The absolute date ranges from the OxCal age-depth model (against Marine20) are also given. As the marine calibration record is more uncertain than IntCal20, the most probable true age for each depth at which a shell sample was obtained is extracted from the terrestrial plant age-depth model.

Marine Shells																	
Lab Ref		Sample Detail	Depth (cm)			δ13X(%, çΠΔB)	14C Age		Modelled Absolute Date (Marine20, Year cal BP)					Mean Modelled Date for this Depth (Year cal BP, Terrestrial Model)	Marine20 14C Age for this Absolute Date		△R	
			Top	Bottom	Average		14C yr BP	±1σ	From (68%)	To (68%)	From (95%)	To (95%)	Mean		14C yr BP	±	14C yr	±1σ
	GrM-27739	*Loripes orbiculatus*	188	192	190	−1.86	3442	22	3154	3048	3204	2987	3097	2531	2936	57	506	61
	GrM-27740	*Loripes orbiculatus*	200	204	202	−1.77	3406	24	3234	3145	3275	3090	3186	2809	3187	57	219	62
	GrM-27741	*Loripes orbiculatus*	208	212	210	−2.47	3490	22	3304	3220	3335	3169	3256	3005	3342	56	148	61
a	GrM-27743	*Loripes orbiculatus*	212	216	214	−1.08	3549	22	3340	3259	3372	3209	3294	3113	3415	58	134	62
	GrM-27744	*Loripes orbiculatus*	*220*	*223*	*222*	*0.00*	*3977*	*24*	*3418*	*3336*	*3475*	*3275*	*3377*	-	-	-	-	-
	GrM-27745	*Loripes orbiculatus*	227	230	229	−0.57	3676	24	3478	3406	3527	3362	3443	3436	3688	58	−12	63
	GrM-27746	*Loripes orbiculatus*	230	235	233	−0.67	3710	24	3517	3444	3564	3401	3483	3525	3767	57	−57	61
	GrM-27749	*Loripes orbiculatus*	240	245	243	0.37	3882	22	3633	3547	3703	3518	3600	3647	3866	57	16	61
	GrM-27750	*Loripes orbiculatus*	245	252	249	1.12	3937	22	3691	3602	3755	3574	3656	3696	3903	57	34	61
a	GrM-27751	*Loripes orbiculatus*	260	265	263	1.06	3986	26	3800	3719	3855	3688	3767	3844	4016	57	−30	63
a	GrM-27757	*Loripes orbiculatus*	270	275	273	0.18	3968	24	3882	3799	3930	3755	3842	3876	4038	58	−70	63
	GrM-27752	*Loripes orbiculatus*	295	300	298	1.26	4231	22	4112	4007	4163	3963	4061	3938	4086	58	146	62
a	GrM-27754	*Loripes orbiculatus*	300	305	303	1.08	4318	22	4158	4050	4203	3992	4098	3951	4090	58	228	62
	GrM-27755	*Loripes orbiculatus*	310	317	314	0.53	4198	24	4222	4096	4303	4039	4167	–	–	–	–	–
	GrM-27756	*Loripes orbiculatus*	317	325	321	1.21	4136	24	4276	4123	4377	4067	4213	–	–	–	–	–

[a] Paired with terrestrial samples.

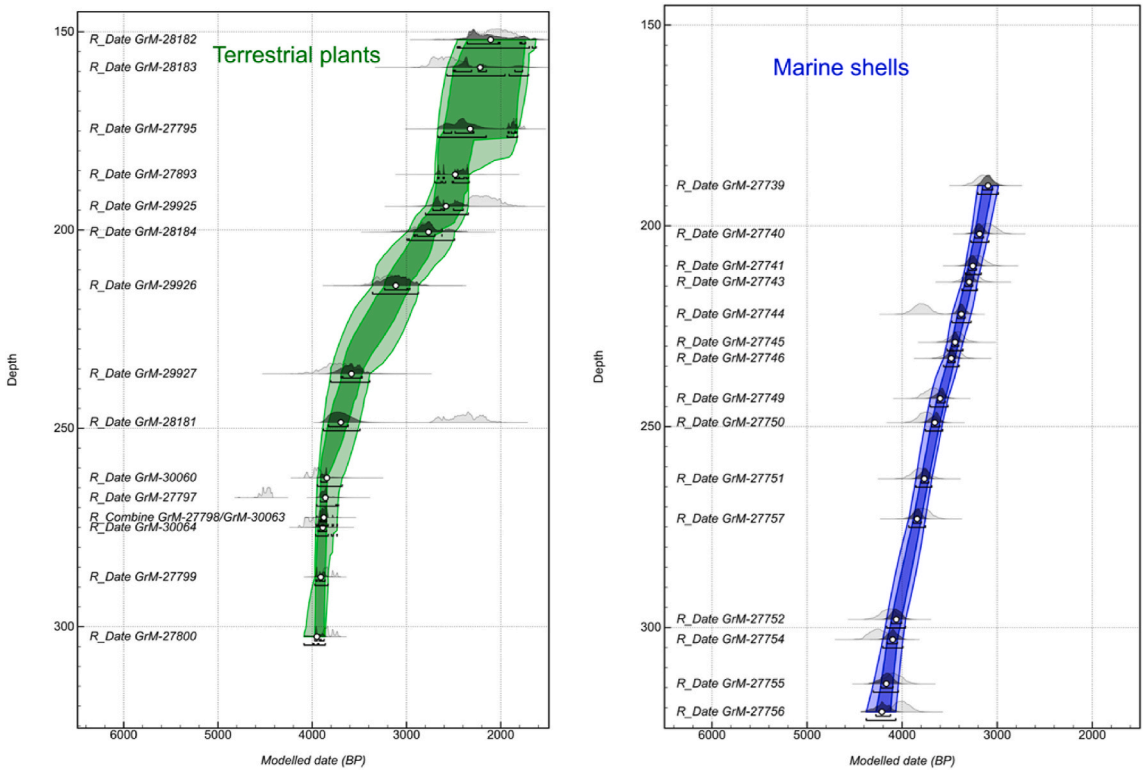

Fig. 5. Age-depth models obtained on the terrestrial plant samples (5a) and on the marine shells (5b) from Puntone, using the P Sequence function in OxCal (see Appendix for code). The 68% and 95% ranges are indicated by the coloured areas (light and dark), and the mean values by the open circles.

Table 6
The values for △R obtained on the paired terrestrial and marine samples in the core as determined by the *deltar* program. The two samples from 273 (272.5) cm depth are not statistically equivalent so their corresponding △R values are calculated independently.

Terrestrial Plants					Marine Shells					Mean Modelled Date for this Depth (Year cal BP, Terrestrial Model)	△R from Reimer and Reimer (2017) deltar Program	
Sample Detail	Depth (cm)	Lab Ref	14C Age		Sample Detail	Depth (cm)	Lab Ref	14C Age				
	Average		14C yr BP	±1σ		Average		yr BP	±		△R	±1σ
Charcoal	214	GrM-29926	2980	110	*Loripes orbiculatus*	214	GrM-27743	3549	22	3113	83	122
Charcoal	263	GrM-30060	3641	26	*Loripes orbiculatus*	263	GrM-27751	3986	26	3844	−114	48
Charcoal	273	GrM-30063	3495	24	*Loripes orbiculatus*	273	GrM-27757	3968	24	3876	12	42
Seeds	273	GrM-27798	3650	26	*Loripes orbiculatus*	273	GrM-27757	3968	24	3876	−147	49
Seeds	303	GrM-27800	3549	26	*Loripes orbiculatus*	303	GrM-27754	4318	22	3951	297	41

given the scarceness of such material in the marine/lagoonal environment in which this mollusc lived (see also data on sediment composition presented in Table 1), and the irrelevance of the potentially associated flux of such carbonate relative to that associated with its species-specific physiology and metabolism.

The complex pathways of carbon in the *Loripes* bacteria system may well be associated with isotopic fractionation, leading to a relative reduction of the concentrations of heavier isotopes in the shells. Whereas shell formation is considered not to be associated with significant isotopic fractionation (McConnaughey and Gillikin, 2008), the bacteria-host pathway may well be so and thus variation in food uptake (bacterial sugar compounds versus inhaled particulate organic carbon) might readily induce changes in the carbon isotopic composition of its shells (Roques et al., 2020). However, such fractionation, if present, is accounted for in the standardised correction of radiocarbon dates (Dee et al., 2020) and thus cannot be held responsible for the observed variability in the MRE values.

One of the potential effects of the variation in environmental conditions over time is a systemic change from a carbon sink to a carbon source, potentially arising from the combination of high salinity, warmer waters and stagnant conditions, which would have reduced the growth of marine vegetation and carbon dioxide gas fluxes (Bolin, 1960). Such a scenario is known to occur where evaporation leads to increased salinity and the concurrent chemical precipitation of calcium carbonate (Dore et al., 2003; Heinsch et al., 2004; Duarte et al., 2008). The obvious question thus arises of whether gas exchange between the atmosphere and the seawater might be so retarded that the carbon isotopic composition of the latter is reduced to such an extent that it

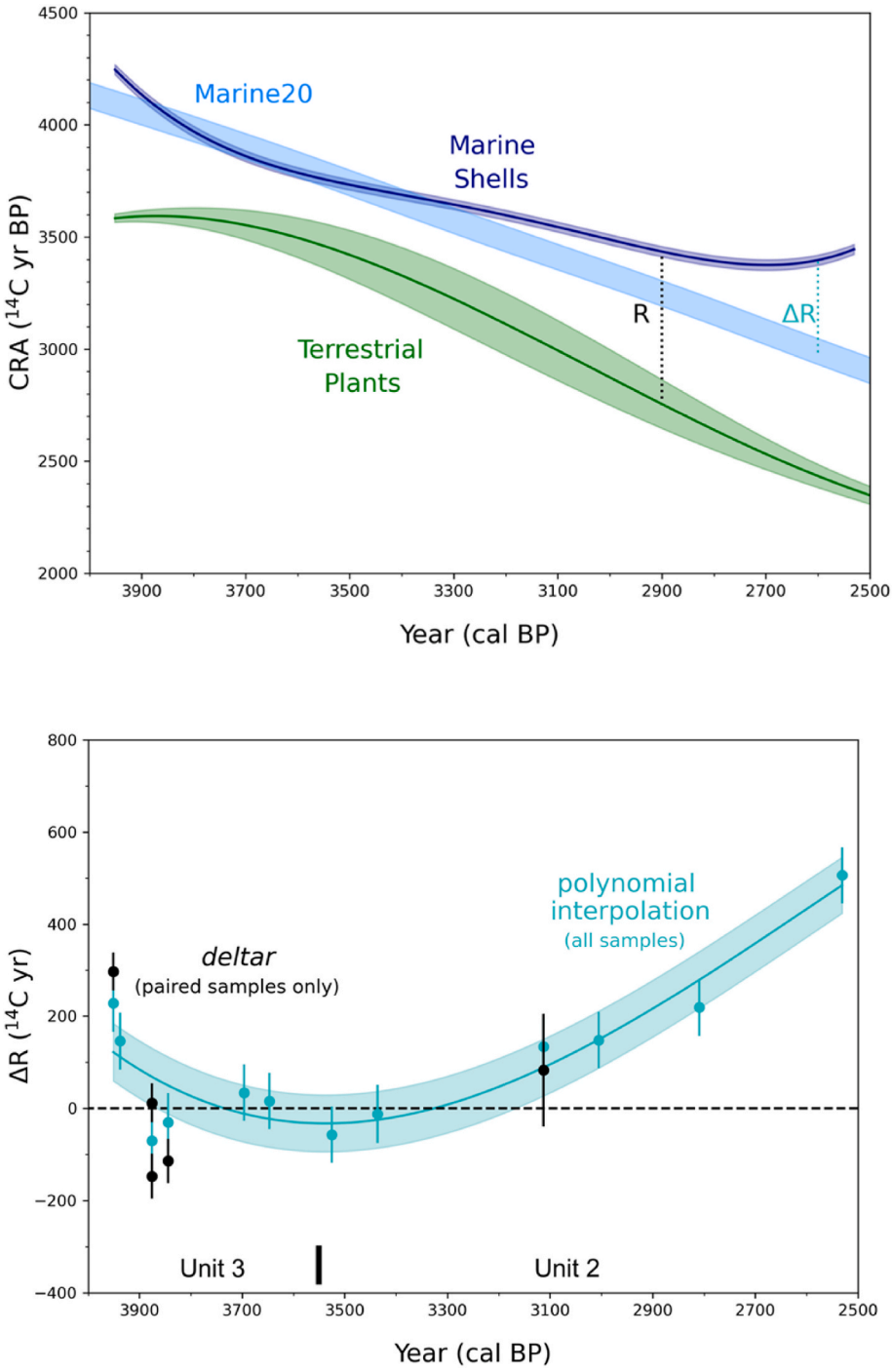

Fig. 6. a) Uncalibrated versus calibrated ages plots for the terrestrial (green) and marine (navy) samples from Puntone. Shown also are Marine20 (light blue) and the origin of R and △R. In each case, the individual points are interpolated using a polynomial function (degree = 4); b) The diachronic variation in △R at Puntone. The estimates obtained from the *deltar* program are shown in black. The estimates obtained from the polynomial interpolation of the marine shell results are given in light blue.

acquires an 'older' ^{14}C signature. Though studies on gas exchange equilibria in shallow, saline lagoonal systems are rare and inconclusive regarding this possible effect (Valero-Garcés et al., 1999; Weber et al., 2018), it is highly unlikely to have played a significant role since all published studies stress the rapidity with which equilibrium is reached between atmospheric and water dissolved carbon dioxide by turbulent processes and molecular diffusion.

A much more plausible cause is the production and uptake by *L. orbiculatis* of 'old carbon' produced by microbial breakdown of autochtonic organic matter (Roth et al., 2023) in the sediment column of coastal systems, like the process encountered in peat bogs (Raghoebarsing et al., 2005; Steinmann et al., 2008), which has been shown to lead to erroneously old ^{14}C dates for submerged *Sphagnum* plants. As published by Kristensen et al. (1995) and confirmed by many subsequent studies (e.g., Migliore et al., 2012), even under truly anaerobic conditions a significant amount of CO_2(aq) is produced by the microbial breakdown of organic matter in the sediment column (described as biologically controlled diagenesis) with methanogenesis as a well-established process (e.g., Konhauser et al., 2011). Methanogenesis is particularly known from anaerobic sediments in coastal marine

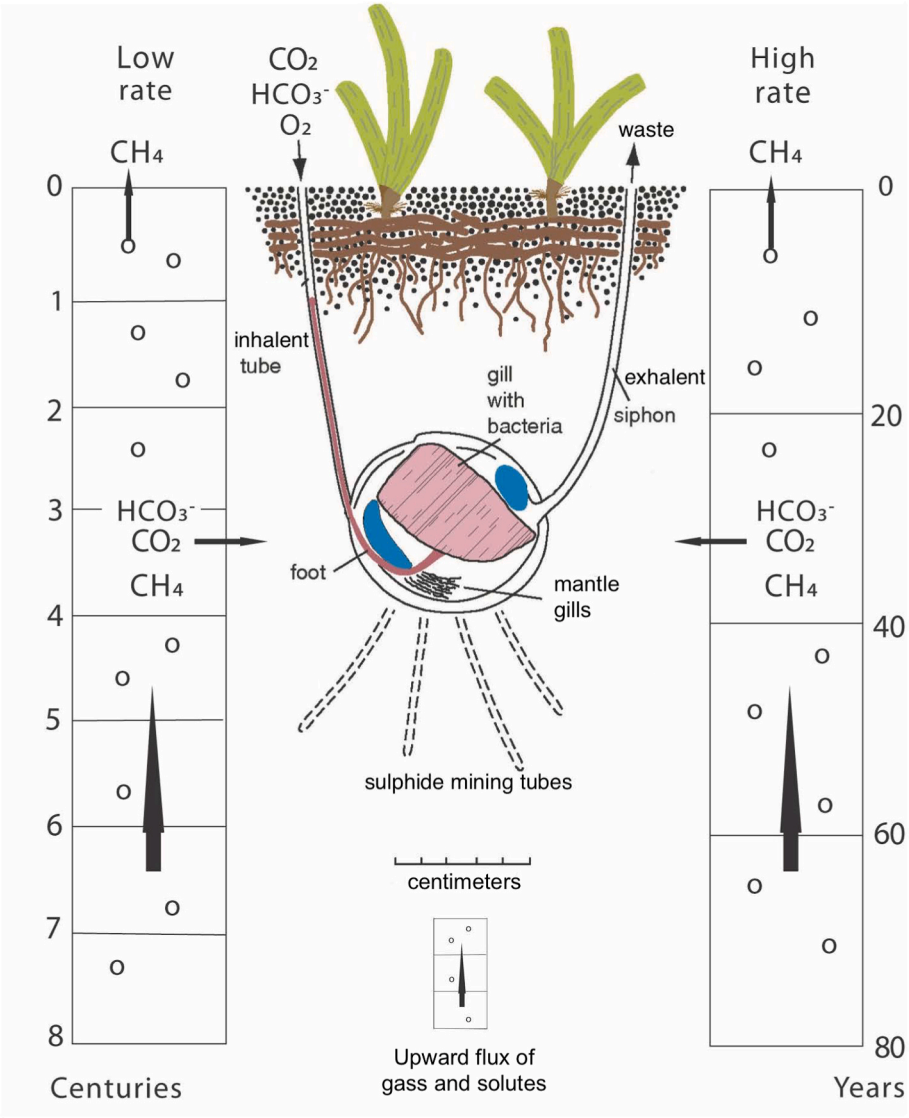

Fig. 7. Carbon pools and fluxes in shallow coastal systems with *Loripes orbiculatus* and with low and high sedimentation rates. Partly after Stanley (2014).

environments and freshwater wetlands. It involves microbial breakdown of organic matter following various and still not fully established pathways (Ferry and Lessner 2008; Fenchel et al., 2012). Three main pathways are distinguished: acetoclastic methanogenesis, which is most active and important in freshwater sediments, in which acetate serves as substrate, producing carbon dioxide and methane, methylotrophic methanogenesis in which methanol or methylamines serve as substrates, producing carbon dioxide and methane, and hydrogenotrophic methanogenesis in which hydrogen is used for the reduction of carbon dioxide to methane. The methane formed is poorly soluble in water, leading to the development of bubbles and an extensively studied upward flux of gaseous methane described as ebullition (Oldenburg and Lewicki 2006; Chanton and Whiting 2009; Cheng et al., 2014). The resulting flux of methane contributes significantly to the global atmospheric methane stocks and explains the attention paid to this methanogenesis and the metabolic processes and microorganisms involved, which is boosted by the greatly enhanced potential of genomic studies (Gilmore et al., 2017) and important role of methane as greenhouse gas (Saunois et al., 2020; Roth et al., 2023). Because of the high solubility of carbon dioxide in water, ebullition plays a lesser role in its exchange between the sediment column and the atmosphere, but its production, notably in methylotrophic methanogenesis leads to a significant flux and relatively high pCO_2 levels in interstitial pore waters in the sediment column (Cai et al., 2000; Upstill-Goddard 2006; Schorn et al., 2022).

Among the various marine-lagoonal ecosystems, seagrass ecosystems count among the relatively poorly studied systems (Al-Haj and Fulweiler, 2020). However, Schorn et al. (2022) produced a detailed and highly relevant study of seagrass meadows in the nearby bay of Fetovaia, Elba (Italy), which very much resemble the seagrass meadows that existed at the Puntone site that we studied. They found that diverse methylotrophic methanogenic archaea caused high methane emissions from the seagrass meadows, implying that in addition carbon dioxide is produced, indeed reflected in high pCO_2 levels in the pore waters of the sediment columns studied in which methanogenesis was found to be an important process. Interestingly, based on both sampling of porewaters and incubation experiments, they found that even in sediment with abundant dead *P. oceanica* seagrass methane was produced, and that methane production in such dead seagrass-dominated sediment was significant up to a depth of 30–45 cm, while at greater depth its production fell back sharply. This high production of methane by microbial breakdown of dead seagrass is ascribed to its high content of methylated compounds, that act as methane precursors.

In anaerobic sediments increased salinity was found to result in increased CO_2(aq) production and a decrease of methanogenesis

(Baldwin et al., 2006). Evidently, the impact of this microbial production on the total stock of CO_2(aq) (and HCO_3^-) available to *L. orbiculatis* shells (and their symbionts) within the sediment column would depend on the depth to which microbial breakdown is active in this column, and on the age of the sediment involved, and on the depth from the lagoon bottom into which the individual molluscl had burrowed. Differences in sedimentation rate thus will have a direct impact on the apparent radiocarbon age of the inorganic carbon pool (CO_2(aq) and HCO_3^-) in the sediment surrounding the molluscs. Major differences in the origin of this pool can be expected between shallow bays and open lagoons with relatively high sedimentation rates, on the one hand, and shallow lagoons to salt marshes with far lower sedimentation rates, on the other hand, with increasing (old) microbial CO_2(aq) and lesser atmospheric carbon dioxide input, because of decreased turbulence, elevated salinity, and increased temperature of the latter systems. The differences are depicted in Fig. 7, showing these two systems and fluxes of the major inorganic carbon compounds, based on the sedimentation rate found for the lithological units 2 and 3, and reported burrowing depths for *L. orbiculatus* (e.g., Stanley 2014).

Together these studies strongly support our hypothesis on the presumed role of 'old carbon' and its uptake by *L. orbiculatus*. According to the definitions used by Roth et al. (2023) this 'old carbon' can be described as autochtonous old carbon, i.e., derived from autochtonic plant material present in the sediment column, and thus having its sedimentation rate-dependent radiocarbon age. A rough estimate of the age of the dissolved carbon dioxide in the pore water at 30–45 cm depth produced by methylotrophic methanogenesis of the autochtonic plant material at that depth, assuming a sedimentation rate of 4 cm/century, would be in the order of 800–1000 years. That methanogenesis indeed leads to a massive flux of ^{14}C depleted methane is well established (Hovland et al., 1993; Adler et al., 2011) and has been extensively described in many studies on the global methane budget (Bouchard et al., 2015; Pohlman et al., 2013.

6. Conclusions

The principal conclusion is that the ΔR value for the mollusc species that we studied (*L. orbiculatus*) is variable over time, its value ranging from slightly negative (ca. −50 years) to ca. 500 years. Extensive analysis of the environmental conditions and sedimentary facies in the area and during the period covered by the Puntone core, showed that none of the usual factors and processes could adequately explain such a dynamic and ultimately enhanced MRE. No evidence was found for relevant increases in 'old' terrestrial carbon input, nor for any 'old' carbon from upwelling seawater. The shift from carbon reservoir to carbon source which very likely resulted from the change from an open marine environment with a productive marine vegetation to a very shallow, less vegetated lagoon/salt marsh, may have been accompanied by a declining influx of atmospheric carbon dioxide into the marine system, because of the declining turbulence, higher salinity, and higher water temperature. Yet, this is also very improbable to have resulted in the major changes in ΔR values we found.

Possibly the most plausible explanation for the offsets is a shift in the relative amount of 'old' carbon released in the form of CO_2/HCO_3^- by microbial decomposition of organic matter in the sediment column in which the mollusc had buried. In simple terms, the impact of this diagenetic CO_2/HCO_3^- flux would depend on the depth to which the individual shell burrowed, the contemporary sedimentation rate and differences in the overall age of the sediment column concerned. The complexity of the carbon fluxes in these coastal systems is impressive as shown by Komada et al. (2022) and further study is needed to substantiate such a hypothesis. Even without such information, it is evident that ^{14}C dates for *L. orbiculatus* shells and other lucinid molluscs from shallow coastal environments are vulnerable to being unreliable dating proxies, which has important implications for studies in which such results were used to establish chronostratigraphies (e.g., Marriner et al., 2005; Vött, 2007; Vacchi et al., 2017; Karymbalis et al., 2022).

Whether the facies-dependent ΔR values are limited to burrowing mollusc species, or they occur in any benthic species where a significant influence from inorganic carbon release by diagenetic microbial decomposition can be expected, is also not clear. This question forms an interesting topic for further study and might lead to a better understanding of the variability of ΔR values obtained for marine fauna from shallow coastal environments. At the same time our results indicate that researchers must be careful when using burrowing mollusc species for radiocarbon dating.

The further study could include a diachronic study of terrestrial plant macroremains, lucinid, and other benthic and pelagic molluscs as well as of benthic and pelagic foraminifers and ostracods in a core from such shallow coastal environment to assess the role of methanogenesis-related carbon dioxide fluxes. This is in fact the main topic of a study that we recently started on a core from a Campanian marine lagoonal sediment complex.

Funding

This research did not receive any specific grant from funding agencies in the public, commercial, or not-for-profit sectors. The INGV-OV laboratories have been financially supported by the EPOS Research Infrastructure through the contribution of the Italian Ministry of University and Research (MUR)

CRediT authorship contribution statement

Jan Sevink: Conceptualization, Data curation, Formal analysis, Investigation, Methodology, Supervision, Writing – original draft, Writing – review & editing. **Michael W. Dee:** Conceptualization, Data curation, Formal analysis, Investigation, Methodology, Supervision, Validation, Writing – review & editing. **Justyna J. Niedospial:** Data curation, Formal analysis, Investigation, Methodology. **Arnoud Maurer:** Data curation, Investigation. **Wim Kuijper:** Data curation, Investigation. **Ilaria Mazzini:** Conceptualization, Data curation, Formal analysis, Investigation, Methodology. **Ilenia Arienzo:** Data curation, Formal analysis, Investigation, Methodology, Visualization. **Rutger L. van Hall:** Data curation, Formal analysis, Investigation.

Declaration of competing interest

The authors declare that they have no known competing financial interests or personal relationships that could have appeared to influence the work reported in this paper.

Data availability

Data will be made available on request.

Appendix A. Supplementary data

Supplementary data to this article can be found online at https://doi.org/10.1016/j.quageo.2024.101505.

References

Adler, M., Eckert, W., Sivan, O., 2011. Quantifying rates of methanogenesis and methanotrophy in Lake Kinneret sediments (Israel) using pore-water profiles. Limnol. Oceanogr. 56 (4), 1525–1535. https://doi.org/10.4319/lo.2011.56.4.1525.

Aerts-Bijma, A.T., Paul, D., Dee, M.W., Palstra, S.W.L., Meijer, H.A.J., 2021. An independent assessment of uncertainty for radiocarbon analysis with the new generation high-yield accelerator mass spectrometers. Radiocarbon 63 (1), 1–22. https://doi.org/10.1017/RDC.2020.101.

Aiello, E., Bartolini, C., Caputo, C., D'Alessandro, L., Panucci, F., Fierro, G., Gnaccolini, M., La Monica, G.B., Palmieri, E., Picazzo, M., Pranzini, E., 1975. Il trasporto litoraneo lungo la costa toscana tra la foce del fiume Magra e i Monti dell'Uccellina. Boll. Soc. Geol. Ital. 94, 1519–1571, 1975.

Alessandri, L., Achino, K.F., Attema, P.A., de Novaes Nascimento, M., Gatta, M., Rolfo, M. F., Sevink, J., Sottili, G., Van Gorp, W., 2019. Salt or fish (or salted fish)? The Bronze Age specialised sites along the Tyrrhenian coast of Central Italy: new insights from Caprolace settlement. PLoS One 14 (11), e0224435. https://doi.org/10.1371/journal.,pone.0224435.

Al-Haj, A.N., Fulweiler, R.W., 2020. A synthesis of methane emissions from shallow vegetated coastal ecosystems. Global Change Biol. 26 (5), 2988–3005. https://doi.org/10.1111/gcb.15046.

Allen, J.A., 1953. Function of the foot in the *Lucinacea (Eulamellibranchia)*. Nature 171 (4364), 1117–1118.

Allen, J.A., 1958. On the basic form and adaptations to habitat in the Lucinacea (Eulamellibranchia). Proc. Royal Soc. B. 241 (684), 421–484.

Alves, E.Q., Macario, K., Ascough, P., Bronk Ramsey, C., 2018. The worldwide marine radiocarbon reservoir effect: definitions, mechanisms, and prospects. Rev. Geophys. 56 (1), 278–305. https://doi.org/10.1002/2017RG000588.

Aranguren, B.M., Cinquegrana, M.R., De Bonis, A., Guarino, V., Morra, V., Pacciarelli, M., 2014. Le strutture e lo scarico di olle del Puntone Nuovo di Scarlino (GR), e i siti costieri specializzati della protostoria mediotirrenica. Riv. Sci. Preist. LXIV, 227–259.

Arienzo, I., Carandente, A., Di Renzo, V., Belviso, P., Civetta, L., D'Antonio, M., Orsi, G., 2013. Sr and Nd isotope analysis at the Radiogenic Isotope Laboratory of the Istituto Nazionale di Geofisica e Vulcanologia Sezione di Napoli—Osservatorio Vesuviano. Rapporti Tecnici INGV 260, 1–18. https://istituto.ingv.it/lingv/produzionescientifica/rapporti-tecnici-ingv/archivio/rapporti-tecnici.

Athersuch, J., Horne, D.J., Whittaker, J.E., 1989. Marine and Brackish Water Ostracods (Superfamilies Cypridacea and Cytheracea): Keys and Notes for the Identification of the Species, vol. 43. Brill Archive.

Baldwin, D.S., Rees, G.N., Mitchell, A.M., Watson, G., Williams, J., 2006. The short-term effects of salinization on anaerobic nutrient cycling and microbial community structure in sediment from a freshwater wetland. Wetlands 26 (2), 455–464. https://doi.org/10.1672/0277-5212 (2006)26[455:TSEOSO]2.0.CO;2.

Beug, H., 2004. Leitfaden der Pollenbestimmung Fur Mitteleuropa und angrenzende Gebiete. Verlag Dr. Friedrich Pfeil, Munchen.

Biserni, G., Van Geel, B., 2005. Reconstruction of Holocene palaeoenvironment and sedimentation history of the Ombrone alluvial plain (South Tuscany, Italy). Rev. Palaeobot. Palynol. 136 (1–2), 16–28. https://doi.org/10.1016/j.revpalbo.2005.04.002.

Bodergat, A.M., Rio, M., Andréani, A.M., 1991. Composition chimique et ornementation de *Cyprideis torosa* (Crustacea, Ostracoda) dans le domaine paralique. Oceanol. Acta 14, 505–514.

Bolin, B., 1960. On the exchange of carbon dioxide between the atmosphere and the sea. Tellus 12 (3), 274–281. https://doi.org/10.3402/tellusa.v12i3.9402.

Booth, J.M., Fusi, M., Marasco, R., Daffonchio, D., 2023. The microbial landscape in bioturbated mangrove sediment: a resource for promoting nature-based solutions for mangroves. Microb.Biotechn. 1584–1602 https://doi.org/10.1111/1751-7915.14273.

Boschetti, T., Venturelli, G., Toscani, L., Barbieri, M., Mucchino, C., 2005. The Bagni di Lucca thermal waters (Tuscany Italy): an example of Ca-SO_4 waters with high Na/Cl and low Ca/SO_4 ratios. J. Hydrol. 307 (1–4), 270–293. https://doi.org/10.1016/j.jhydrol.2004.10.015.

Bouchard, F., Laurion, I., Prėskienis, V., Fortier, D., Xu, X., Whiticar, M.J., 2015. Modern to millennium-old greenhouse gases emitted from ponds and lakes of the Eastern Canadian Arctic (Bylot Island, Nunavut). Biogeosci 12 (23), 7279–7298. https://doi.org/10.5194/bg-12-7279-2015.

Butler, S., Bailey, T.R., Lear, C.H., Curry, G.B., Cherns, L., McDonald, I., 2015. The Mg/Ca–temperature relationship in brachiopod shells: Calibrating a potential palaeoseasonality proxy. Chem. Geol. 397, 106–117. https://doi.org/10.1016/j.chemgeo.2015.01.009.

Cai, W.J., Zhao, P., Wang, Y., 2000. pH and pCO2 microelectrode measurements and the diffusive behavior of carbon dioxide species in coastal marine sediments. Marine Chem 70 (1–3), 133–148. https://doi.org/10.1016/S0304-4203(00)00017-7.

Cappuccini, L., 2011. Il litorale tirrenico a sud di Populonia in epoca etrusca. In: Paoletti, O. (Ed.), La Corsica e Populonia. Atti del 28 Convegno di Studi Etruschi ed Italici: Bastia, Aléria, Piombino, Populonia, pp. 567–590, 25-29 ottobre 2011.

Cardini, U., Marín-Guirao, L., Montilla, L.M., Marzocchi, U., Chiavarini, S., Rimauro, J., Quero, G.M., Petersen, J.M., Procaccini, G., 2022. Nested interactions between chemosynthetic lucinid bivalves and seagrass promote ecosystem functioning in contaminated sediments. Front. Pl. Sci. 13. https://doi:10.3389/fpls.2022.918675.

Chanton, J.P., Whiting, G.J., 2009. Trace gas exchange in freshwater and coastal marine environments: ebullition and transport by plants. Biogenic trace gases: measuring emissions from soil and wate. In: Matson, P.A., Harris, R.C. (Eds.), Biogenic Trace Gases: Measuring Emissions from Soil and Water. Blackwell Science, pp. 98–125, 2009.

Cheng, C.H., Huettel, M., Wildman, R.A., 2014. Ebullition-enhanced solute transport in coarse-grained sediments. Limnol. Oceanogr. 59 (5), 1733–1748. https://doi.org/10.4319/lo.2014.59.5.1733.

Cornamusini, G., 2002. Compositional evolution of the Macigno Fm. Of southern Tuscany along a transect from the Tuscan coast to the Chianti hills. Boll. Soc. Geol. Ital. 1, 365–374.

Costantini, E.A., Fantappié, M., L'Abate, G., 2013. Climate and pedoclimate of Italy. In: Costantini, E.A., Dazzi, C. (Eds.), The Soils of Italy. Springer Science & Business Media, Springer, Dordrecht, pp. 19–37.

De Deckker, P., Lord, A., 2017. *Cyprideis torosa*: a model organism for the Ostracoda? J. Micropalaeontol. 36, 3–6. https://doi:10.1144/jmpaleo2016-100.

Dee, M.W., Palstra, S.W.L., Aerts-Bijma, A.T., Bleeker, M.O., De Bruijn, S., Ghebru, F., Jansen, H.G., Kuitems, M., Paul, D., Richie, R.R., Spriensma, J.J., Scifo, A., Van Zonneveld, D., Verstappen-Dumoulin, B.M.A.A., Wietzes-Land, P., Meijer, H.A.J., 2020. Radiocarbon dating at Groningen: new and updated chemical pretreatment procedures. Radiocarbon 62 (1), 63–74. https://doi.org/10.1017/RDC.2019.101.

Deines, P., Goldstein, S.L., Oelkers, E.H., Rudnick, R.L., Walter, L.M., 2003. Standards for publication of isotopic ratio and chemical data in Chemical Geology. Chem. Geol. 202, 1–4. https://doi.org/10.1016/j.chemgeo.2003.08.003.

Deneke, E., Gunther, K., 1981. Petrography and arrangement of Tertiary graywacke and sandstone sequences of the Northern Apennines. Sediment. Geol. 28 (3), 189–230. https://doi.org/10.1016/0037-0738(81)90065-8.

Dickin, A.P., 2005. Radiogenic Isotope Geology. Cambridge University Press, Cambridge.

Dinelli, E., Lucchini, F., Mordenti, A., Paganelli, L., 1999. Geochemistry of Oligocene–Miocene sandstones of the northern Apennines (Italy) and evolution of chemical features in relation to provenance changes. Sediment. Geol. 127 (3–4), 193–207. https://doi.org/10.1016/S0037-0738(99)00049-4.

Dore, J.E., Lukas, R., Sadler, D.W., Karl, D.M., 2003. Climate-driven changes to the atmospheric CO2 sink in the subtropical North Pacific Ocean. Nature 424 (6950), 754–757. https://doi:10.1038/nature01885.

Duarte, C.M., Prairie, Y.T., Montes, C., Cole, J.J., Striegl, R., Melack, J., Downing, J.A., 2008. CO2 emissions from saline lakes: a global estimate of a surprisingly large flux. J. Geophys. Res.: Biogeosci. 113 (G4) https://doi.org/10.1029/2007JG000637.

Fægri, K., Iversen, J., 1989. In: Fægri, K., Kaland, P.E., Krzywinski, K. (Eds.), Textbook of Pollen Analysis, fourth ed. Wiley and Sons, New York.

Faure, G., 1986. Principles of Isotope Geology. John Wiley & Sons, Ltd.

Fenchel, T., King, G.M., Blackburn, T.H., 2012. Bacterial Biogeochemistry: the Ecophysiology of Mineral Cycling, third ed. Academic press.

Ferry, J.G., Lessner, D.J., 2008. Methanogenesis in marine sediments. Ann. New York Acad. Sci. 1125 (1), 147–157. https://doi.org/10.1196/annals.1419.007.

Gilmore, S.P., Henske, J.K., Sexton, J.A., Solomon, K.V., Seppälä, S., Yoo, J.I., Huyett, L. M., Pressman, A., Cogan, J.Z., Kivenson, V., Peng, X., 2017. Genomic analysis of methanogenic archaea reveals a shift towards energy conservation. BMC Genom. 18 (1), 1–14. https://doi.org/10.1186/s12864-017-4036-4.

Giroldini, P., 2012. Between land and sea: a GIS based settlement analysis of the ancient coastal Lagoon of Piombino (Tuscany, Italy). eTopoi 3, 383–389.

Heaton, T., Köhler, P., Butzin, M., Bard, E., Reimer, R., Austin, W., Skinner, L., Ramsey, C.B., Grootes, P.M., Hughen, K.A., Kromer, B., Reimer, P.J., Adkins, J., Burke, A., Cook, M.S., Olsen, J., Skinner, L.C., 2020. Marine20—the marine radiocarbon age calibration curve (0–55,000 cal BP). Radiocarbon 62, 779–820. https://doi.org/10.1017/RDC.2020.68.

Heaton, T.J., Bard, E., Ramsey, C.B., Butzin, M., Hatté, C., Hughen, K.A., Köhler, P., Reimer, P.J., 2023. A response to community questions on the Marine20 radiocarbon age calibration curve: marine reservoir ages and the calibration of 14C samples from the oceans. Radiocarbon 65, 247–273. https://doi.org/10.1017/RDC.2022.66.

Heinsch, F.A., Heilman, J.L., McInnes, K.J., Cobos, D.R., Zuberer, D.A., Roelke, D.L., 2004. Carbon dioxide exchange in a high marsh on the Texas Gulf Coast: effects of freshwater availability. Agric. For. Meteorol. 125 (1–2), 159–172. https://doi.org/10.1016/j.agrformet.2004.02.007.

Heip, C., 1976. The life-cycle of *Cyprideis torosa* (Crustacea, Ostracoda). Oecologia 24, 229–245. https://doi:10.1007/BF00345475.

Henderson, P.A., 1990. Freshwater Ostracods: Keys and Notes for the Identification of the Species, New Series 42. Linnean Society of London and the Estuarine and Coastal Sciences Association, Leiden.

Honkoop, P.J.C., Berghuis, E.M., Holthuijsen, S., Lavaleye, M.S.S., Piersma, T., 2008. Molluscan assemblages of seagrass-covered and bare intertidal flats on the Banc d'Arguin, Mauritania, in relation to characteristics of sediment and organic matter. Neth. J. Sea Res. 60, 235–243. https://doi.org/10.1016/j.seares.2008.07.005.

Hovland, M., Judd, A.G., Burke, R.A., 1993. The global flux of methane from shallow submarine sediments. Chemosphere 26 (1–4), 559–578. https://doi.org/10.1016/0045-6535(93)90442-8.

Immenhauser, A., Schoene, B.R., Hoffmann, R., Niedermayr, A., 2016. Mollusc and brachiopod skeletal hard parts: Intricate archives of their marine environment. Sedimentol 63 (1), 1–59. https://doi.org/10.1111/sed.12231.

Jilbert, T., Cowie, G., Lintumäki, L., Jokinen, S., Asmala, E., Sun, X., Morth, C.M., Norkko, A., Humborg, C., 2021. Anthropogenic inputs of terrestrial organic matter influence carbon loading and methanogenesis in coastal Baltic Sea sediments. Fr. Earth Sci. 9, 716416 https://doi.org/10.3389/feart.2021.716416.

Karymbalis, E., Tsanakas, K., Cundy, A., Iliopoulos, G., Papadopoulou, P., Protopappas, D., Gaki-Papanastassiou, K., Papanastassiou, D., Batzakis, D.-V., Kotinas, V., Maroukian, H., 2022. Late Holocene palaeogeographic evolution of the Lihoura coastal plain, Pteleos Gulf, Central Greece. Quat. Int. 638, 70–83. https://doi.org/10.1016/j.quaint.2021.12.007.

Komada, T., Bravo, A., Brinkmann, M.T., Lu, K., Wong, L., Shields, G., 2022. "Slow" and "fast" in blue carbon: Differential turnover of allochthonous and autochthonous organic matter in minerogenic salt marsh sediments. Limnol. Oceanogr. 67, S133–S147. https://doi.org/10.1002/lno.12090.

Konhauser, K.O., Gingras, M.K., Kappler, A., 2011. Sediment diagenesis–biologically controlled. In: Reitner, J., Thiel, V. (Eds.), Encyclopedia of Geobiology. Encyclopedia of Earth Sciences Series. Springer, Dordrecht. https://doi.org/10.1007/978-1-4020-9212-1_179.

Kristensen, E., Ahmed, S.I., Devol, A.H., 1995. Aerobic and anaerobic decomposition of organic matter in marine sediment: which is fastest? Limnol. Oceanogr. 40 (8), 1430–1437. https://doi.org/10.4319/lo.1995.40.8.1430.

Lambeck, K., Antonioli, F., Purcell, A., Silenzi, S., 2004. Sea-level change along the Italian coast for the past 10,000 yr. Quat. Sci. Rev. 23 (14–15), 1567–1598. https://doi.org/10.1016/j.quascirev.2004.02.009.

Lindauer, S., Hadden, C.S., Macario, K., Guilderson, T.P., 2022. Marine biogenic carbonates and radiocarbon—a retrospective on shells and corals with an outlook on

challenges and opportunities. Radiocarbon 64 (4), 689–704. https://doi.org/10.1017/RDC.2021.93.
Liu, Y.W., Aciego, S.M., Wanamaker, A.D., 2015. Environmental controls on the boron and strontium isotopic composition of aragonite shell material of cultured *Arctica islandica*. Biogeosci 12 (11), 3351–3368. https://doi.org/10.5194/bg-12-3351-2015.
Marriner, N., Morhange, C., Boudagher-Fadel, M., Bourcier, M., Carbonel, P., 2005. Geoarchaeology of Tyre's ancient northern harbour, Phoenicia. J. Archaeol. Sci. 32 (9), 1302–1327. https://doi.org/10.1016/j.jas.2005.03.019.
Masetti, G., Da Prato, S., Menichini, M., Raco, B., Lavorini, G., Positano, P., Puglici, A., 2017. Dal modello concettuale al modello numerico: il caso di studio del sistema acquifero di Follonica (GR, Toscana meridionale). Rend. Online Soc. Geol. It. 42, 54–58. https://doi:10.3301/ROL.2017.13.
Mazzini, I., Rossi, V., Da Prato, S., Ruscito, V., 2017. Ostracods in archaeological sites along the Mediterranean coastlines: three case studies from the Italian peninsula. In: Williams, M., et al. (Eds.), The Archaeological and Forensic Applications of Microfossils: A Deeper Understanding of Human History. The Micropalaeontological Society, London, pp. 121–142. https://doi.org/10.1144/TMS7.7.
Mazzini, I., Aiello, G., Frenzel, P., Pint, A., 2022. Marine and marginal marine Ostracoda as proxies in geoarchaeology. Mar. Micropaleontol. 174, 102054 https://doi.org/10.1016/j.marmicro.2021.102054.
McCaffrey, M.A., Lazar, B., Holland, H.D., 1987. The evaporation path of sea water and the coprecipitation of Br- and K+ with halite. J. Sediment. Petrol. 57, 928–937. https://doi.org/10.1306/212F8CAB-2B24-11D7-8648000102C1865D.
McConnaughey, T.A., Gillikin, D.P., 2008. Carbon isotopes in mollusk shell carbonates. Geo Mar. Lett. 28, 287–299. https://doi10.1007/s00367-008-0116-4.
Migliore, G., Alisi, C., Sprocati, A.R., Massi, E., Ciccoli, R., Lenzi, M., Wang, A., Cremisini, C., 2012. Anaerobic digestion of macroalgal biomass and sediments sourced from the Orbetello lagoon. Italy. Biomass Bioenergy 42, 69–77. https://doi.org/10.1016/j.biombioe.2012.03.030.
Moore, P.D., Webb, J.A., Collison, M.E., 1991. Pollen Analysis. Blackwell Scient. Publ.
Nisi, B., Buccianti, A., Vaselli, O., Perini, G., Tassi, F., Minissale, A., Montegrossi, G., 2008. Hydrogeochemistry and strontium isotopes in the Arno River Basin (Tuscany, Italy): constraints on natural controls by statistical modeling. J. Hydrol. 360 (1–4), 166–183. https://doi.org/10.1016/j.jhydrol.2008.07.030.
Oldenburg, C.M., Lewicki, J.L., 2006. On leakage and seepage of CO2 from geologic storage sites into surface water. Environm. Geol. 50, 691–705. https://doi.org/10.1007/s00254-006-0242-0.
Pennisi, M., Bianchini, G., Kloppmann, W., Muti, A., 2009. Chemical and isotopic (B, Sr) composition of alluvial sediments as archive of a past hydrothermal outflow. Chem. Geol. 266 (3–4), 114–125. https://doi.org/10.1016/j.chemgeo.2009.05.017.
Petchey, F., Ulm, S., David, B., McNiven, I.J., Asmussen, B., Tomkins, H., Richards, T., Rowe, C., Leavesley, M., Mandui, H., Stanisic, J., 2012. Radiocarbon marine reservoir variability in herbivores and deposit-feeding gastropods from an open coastline, Papua New Guinea. Radiocarbon 54 (3–4), 967–978. https://doi.org/10.1017/S0033822200047603.
Pohlman, J.W., Riedel, M., Bauer, J.E., Canuel, E.A., Paull, C.K., Lapham, L., Grabowski, K.S., Coffin, R.B., Spence, G.D., 2013. Anaerobic methane oxidation in low-organic content methane seep sediments. Geochim. Cosmoch. Acta 108, 184–201. https://doi.org/10.1016/j.gca.2013.01.022.
Positano, P., Nannucci, M., 2017. The H2O20 FREEWAT participated approach for the Follonica-Scarlino aquifer case study. A common space to generate shared knowledge on the value of water. Acque Sotterranee–Ital., Groundwater 6 (3/149), 27–38. https://doi:10.7343/as-2017-290.
Poulain, C., Gillikin, D.P., Thébault, J., Munaron, J.M., Bohn, M., Robert, R., Paulet, Y. M., Lorrain, A., 2015. An evaluation of Mg/Ca, Sr/Ca, and Ba/Ca ratios as environmental proxies in aragonite bivalve shells. Chem. Geol. 396, 42–50. https://doi.org/10.1016/j.chemgeo.2014.12.019.
Quarta, G., Maruccio, L., D'Elia, M., Calcagnile, L., 2021. Radiocarbon dating of marine samples: Methodological Aspects, applications and case studies. Water 13 (7), 986. https://doi.org/10.3390/w13070986.
Raco, B., Buccianti, A., Corongiu, M., Lavorini, G., Macera, P., Manetti, F., Mari, R., Masetti, G., Menichetti, S., Nisi, B., Protano, G., Romanelli, S., 2015. GEOBASI: the geochemical database of Tuscany region (Italy). Acque Sotterranee, it. J. Groundwater 4 (1), 7–18. https://doi.org/10.7343/as-100-15-0127.
Raghoebarsing, A.A., Smolders, A.J.P., Schmid, M.C., Rijpstra, W.I.C., Wolters-Arts, M., Derksen, J., Jetten, M.S.M., Schouten, S., Damste, J.S.S., Lamers, L.P.M., Roelofs, J. G.M., Den Camp, H., Strous, M., 2005. Methanotrophic symbionts provide carbon for photosynthesis in peat bogs. Nature 436, 1153–1156. https://doi:10.1038/nature03802.
Ramsey, C.B., 1995. Radiocarbon calibration and analysis of stratigraphy: the OxCal program. Radiocarbon 37 (2), 425–430. https://doi.org/10.1017/S0033822200030903.
Reimer, P.J., Reimer, R.W., 2001. A marine reservoir correction database and on-line interface. Radiocarbon 43 (2A), 461–463. https://doi.org/10.1017/S0033822200038339.
Reimer, R.W., Reimer, P.J., 2017. An online application for ΔR calculation. Radiocarbon 59 (5), 1623–1627. https://doi.org/10.1017/RDC.2016.117.
Reimer, P.J., Austin, W.E.N., Bard, E., Bayliss, A., Blackwell, P.G., Bronk Ramsey, C., Butzin, M., Cheng, H., Edwards, R.L., Friedrich, M., Grootes, P.M., Guilderson, T.P., Hajdas, I., Heaton, T.J., Hogg, A.G., Hughen, K.A., Kromer, B., Manning, S.W., Muscheler, R., Palmer, J.G., Pearson, C., Van der Plicht, J., Reimer, R.W., Richards, D.A., Scott, E.M., Southon, J.R., Turney, C.S.M., Wacker, L., Adolphi, F., Buntgen, U., Capano, M., Fahrni, S.M., Fogtmann-Schulz, A., Friedrich, R., Kohler, P., Kudsk, S., Miyake, F., Olsen, J., Reinig, F., Sakamoto, M., Sookdeo, A., Talamo, S., 2020. The IntCal20 Northern Hemisphere radiocarbon age calibration curve (0–55 cal kBP). Radiocarbon 62 (4), 725–757. https://doi.org/10.1017/RDC.2020.41.
Roques, C., Grousset, E., Troussellier, M., Hermet, S., Le Carrer, J., Sar, C., Caro, A., 2020. A trade-off between mucocytes and bacteriocytes in *Loripes orbiculatus* gills (Bivalvia, Lucinidae): a mixotrophic adaptation to seasonality and reproductive status in a symbiotic species? Mar. Biol. 167, 1–16. https://doi.org/10.1007/s00227-020-03768-w.
Rossi, F., Colao, E., Martinez, M.J., Klein, J.C., Carcaillet, F., Callier, M.D., De Wit, R., Caro, A., 2013. Spatial distribution and nutritional requirements of the endosymbiont-bearing bivalve *Loripes lacteus* (sensu Poli, 1791) in a Mediterranean *Nanozostera noltii* (Hornemann) meadow. J. Exp. Mar. Biol. Eco 440, 108–115. https://doi.org/10.1016/j.jembe.2012.12.010.
Roth, F., Broman, E., Sun, X., Bonaglia, S., Nascimento, F., Prytherch, J., Brüchert, V., Lundevall Zara, M., Brunberg, M., Geibel, M.C., Humborg, C., 2023. Methane emissions offset atmospheric carbon dioxide uptake in coastal macroalgae, mixed vegetation and sediment ecosystems. Nature Commun 14 (1), 1–11. https://doi.org/10.1038/s41467-022-35673-9.
Saunois, M., Stavert, A.R., Poulter, B., Bousquet, P., Canadell, J.G., Jackson, R.B., Raymond, P.A., Dlugokencky, E.J., Houweling, S., Patra, P.K., Ciais, P., 2020. The global methane budget 2000–2017. Earth system Sci. Data 12 (3), 1561–1623. https://doi.org/10.5194/essd-12-1561-2020.
Schorn, S., Ahmerkamp, S., Bullock, E., Weber, M., Lott, C., Liebeke, M., Lavik, G., Kuypers, M.M., Graf, J.S., Milucka, J., 2022. Diverse methylotrophic methanogenic archaea cause high methane emissions from seagrass meadows. Proc. Nat. Acad. Sci. 119 (9) https://doi.org/10.1073/pnas.2106628119.
Sevink, J., Beemster, J., Van Stiphout, T., 1986. Soil Survey and Land Evaluation of the Grosseto Area. University of Amsterdam, Amsterdam.
Sevink, J., De Neef, W., Alessandri, L., Van Hall, R.L., Ullrich, B., Attema, P.A., 2020. Protohistoric briquetage at Puntone (Tuscany, Italy): principles and processes of an industry based on the leaching of saline lagoonal sediments. Geoarchaeol. Vol.36 (1) 54-71. https://doi:10.1002/gea.21820.
Sevink, J., Muyzer, G., Arienzo, I., Mormone, A., Piochi, M., Alessandri, L., van Hall, R.L., Palstra, S.W.L., Dee, M.W., 2021. The protohistoric briquetage at Puntone (Tuscany, Italy): a multidisciplinary attempt to unravel its age and role in the salt supply of Early States in Tyrrhenian Central Italy. J. Archaeol. Sci. Rep. 38, 103055 https://doi.org/10.1016/j.jasrep.2021.103055.
Shao, Y., Farkaš, J., Mosley, L., Tyler, J., Wong, H., Chamberlayne, B., Raven, M., Samanta, M., Holmden, C., Gillanders, B.M., Kolevica, A., Eisenhauer, A., 2021. Impact of salinity and carbonate saturation on stable Sr isotopes (δ88/86Sr) in a lagoon-estuarine system. Geochim. Cosmochim. Acta. https://doi.org/10.1016/j.gca.2020.11.014.
Stanley, S.M., 2014. Evolutionary radiation of shallow-water Lucinidae (Bivalvia with endosymbionts) as a result of the rise of seagrasses and mangroves. Geol. 42 (9), 803–806. https://doi.org/10.1130/G35942.1.
Steinmann, P., Eilrich, B., Leuenberger, M., Burns, S.J., 2008. Stable carbon isotope composition and concentrations of CO_2 and methane in the deep catotelm of a peat bog. Geochim. Cosmochim. Acta 72 (24), 6015–6026. https://doi.org/10.1016/j.gca.2008.09.024.
Taylor, J.D., Glover, E.A., 2000. Functional anatomy, chemosymbiosis and evolution of the Lucinidae. Geol. Soc. Lond. Spec. Publ. 177 (1), 207–225. https://doi.org/10.1144/GSL.SP.2000.177.01.12.
Taylor, J.D., Glover, E.A., 2006. Lucinidae (Bivalvia) – the most diverse group of chemosymbiotic molluscs. Zool. J. Linnean Soc. 148, 421–438. https://doi:10.1111/j.1096-3642.2006.00261.x.
Taviani, M. & Correggiari, A. Pers. Comms. ΔR values retrieved for Central Tyrrhenian Sea from http://calib.org/marine/.
Teal, L.R., Bulling, M.T., Parker, E.R., Solan, M., 2008. Global patterns of bioturbation intensity and mixed depth of marine soft sediments. Aquat. Biol. 2 (3), 207–218. https://doi.org/10.3354/ab00052.
Upstill-Goddard, R.C., 2006. Air–sea gas exchange in the coastal zone. Estuar. Coast Shelf Sci. 70 (3), 388–404. https://doi.org/10.1016/j.ecss.2006.05.043.
Vacchi, M., Ghilardi, M., Spada, G., Currás, A., Robresco, S., 2017. New insights into the sea-level evolution in Corsica (NW Mediterranean) since the late Neolithic. J. Archaeol. Sci. Rep. 12, 782–793. https://doi.org/10.1016/j.jasrep.2016.07.006.
Valero-Garcés, B.L., Delgado-Huertas, A., Ratto, N., Navas, A., 1999. Large 13C enrichment in primary carbonates from Andean Altiplano lakes, northwest Argentina. Earth Planet Sci. Lett. 171 (2), 253–266. https://doi.org/10.1016/S0012-821X(99)00150-8.
Van der Geest, M., Van Gils, J.A., Van der Meer, J., Olff, H., Piersma, T., 2011. Suitability of calcein as an in situ growth marker in burrowing bivalves. J. Exp. Mar. Biol. Ecol. 399 (1), 1–7. https://doi.org/10.1016/j.jembe.2011.01.003.
Van Der Heide, T., Govers, L.L., De Fouw, J., Olff, H., Van Der Geest, M., Van Katwijk, M. M., Piersma, T., Van den Koppel, J., Silliman, B.R., Van Gils, J.A., 2012. A three-stage symbiosis forms the foundation of seagrass ecosystems. Science 336 (6087), 1432–1434. https://doi:10.1126/science.1219973.
Vött, A., 2007. Relative sea level changes and regional tectonic evolution of seven coastal areas in NW Greece since the mid-Holocene. Quat. Sci. Rev. 26, 894–919. https://doi.org/10.1016/j.quascirev.2007.01.004.
Weber, U.W., Cook, P.G., Brennwald, M.S., Kipfer, R., Stieglitz, T.C., 2018. A novel approach to quantify air–water gas exchange in shallow surface waters using high-resolution time series of dissolved atmospheric gases. Envir. Sci. Technol. 53 (3), 1463–1470. https://doi.org/10.1021/acs.est.8b05318.
Whiticar, M.J., 2002. Diagenetic relationships of methanogenesis, nutrients, acoustic turbidity, pockmarks and freshwater seepages in Eckernförde Bay. Mar. Geol. 182 (1–2), 29–53. https://doi.org/10.1016/S0025-3227(01)00227-4.

Williams, R.G., Follows, M.J., 2011. Ocean Dynamics and the Carbon Cycle: Principles and Mechanisms. Cambridge University Press.

Yuen, B., Polzin, J., Petersen, J.M., 2019. Organ transcriptomes of the lucinid clam *Loripes orbiculatus* (Poli, 1791) provide insights into their specialised roles in the biology of a chemosymbiotic bivalve. BMC Genom. 20 (1), 1–14. https://doi.org/10.1186/s12864-019-6177-0.

Zauner, S., Vogel, M., Polzin, J., Yuen, B., Mußmann, M., El-Hacen, E.H.M., Petersen, J. M., 2022. Microbial communities in developmental stages of lucinid bivalves. ISME Commun 2 (1), 1–10. https://doi.org/10.1038/s43705-022-00133-4.

Zeebe, R.E., 2012. History of seawater carbonate chemistry, atmospheric CO_2, and ocean acidification. Annu. Rev. Earth Planet Sci. 40, 141–165. https://doi.org/10.1146/annurev-earth-042711-105521.